SEMMELWEIS EGYETEM

DOKTORI ISKOLA

Ph.D. értekezések

3519.

MAJOR MARTIN

Fogorvostudományi kutatások
című program

Programvezető: Dr. Varga Gábor, egyetemi tanár

Témavezető: Dr. Szabó György, egyetemi tanár

THE ROLE OF PLATELET-RICH FIBRIN (PRF) IN POSTOPERATIVE HEALING IN ORAL AND MAXILLOFACIAL SURGERY: CLINICAL, HISTOLOGICAL AND IMAGING APPROACHES

PhD Thesis

Martin Major

Doctoral School of Clinical Medicine

Semmelweis University

Supervisor: György Szabó, MD, D.Sc

Official reviewers: Katalin Nagy, DMD, D.Sc.
Szabolcs Gyulai- Gaál, DMD Ph.D

Head of the Complex Examination Committee:

Gábor Gerber, DMD, D.Sc.

Members of the Complex Examination Committee:

Árpád Joób-Fancsaly, DMD, D.Sc.
Ákos Nagy, DMD, Ph.D.

Budapest

2026

Table of Contents

List of Abbreviations **.....6**

1. Introduction 8

1.1. General Concepts of Wound Healing 8

Definition and Phases of Wound Healing 8

1.2. PRF and its Role in Regenerative Surgery 9

1.2.1. Platelet Rich Fibrin (PRF) 9

1.2.2. Biological Mechanism of Action 10

1.2.3. PRF variants 13

1.2.4. Clinical Relevance in Oral and Maxillofacial Surgery 16

1.3. 3D Facial Scanning in Oral and Maxillofacial Surgery 23

2. Objectives 27

3. Methods 28

3.1. Validation of a 3D Facial Scanner for Craniofacial Anthropometry 29

3.1.1. Study Participants 29

3.1.2. Examiners 29

3.1.3. Three-Dimensional Imaging and Measurement Protocol 30

3.1.4. Time Analysis 34

3.1.5. Statistical Analysis 35

3.2. Randomized Controlled Clinical Trial: The Effect of PRF on Postoperative Outcomes after Apicoectomy 36

3.2.1. Study Design 36

3.2.2. Participants 36

3.2.3. Eligibility Criteria 37

3.2.4. Ethical Approval and Consent 38

3.2.5. Trial Registration and Informed Consent 38
3.2.6. Randomization and Allocation Concealment 39
3.2.7. Blinding 39
3.2.8. Surgical Procedure 40
3.2.9. Postoperative Care 41
3.2.10. Outcome Measures 42
3.2.11. Three-Dimensional Image Acquisition and Analysis 43
3.2.12. Statistical Analysis 44
3.2.12.1. Normality Testing 44
3.2.12.2. Between-Group Comparisons 44
3.2.12.3. Within-Group Comparisons 45
3.2.12.4. Correlation Analysis 45
3.2.12.5. Analytical Approach 46
3.3. Case Report: Composite Use of A-PRF and Albumin-Coated Allograft in a Patient with Gorlin–Goltz Syndrome 47
3.3.1. Detailed Case Description 47
4. Results 54
4.1. Validation of a 3D Facial Scanner for Craniofacial Anthropometry 54
4.2. Randomized Controlled Clinical Trial: The Effect of PRF on Postoperative Outcomes after Apicoectomy 65
4.2.1. Baseline Characteristics 65
4.2.2. Postoperative Quality of Life 67
4.2.3. Postoperative Pain Assessment 69
4.2.4. Postoperative Swelling 70
4.2.5. Correlation Analysis Results 70
4.2.6. Adverse Events 71
4.3. Case Report: Composite Use of A-PRF and Albumin-Coated Allograft in a Patient with Gorlin–Goltz Syndrome 71

5. Discussion 76

5.1. Overview and Principal Findings 76

5.2. Interpretation of Findings in the Context of the Literature 77

5.2.1. Clinical Interpretation of 3D Scanner Validation Results 77

5.2.2. Effect of PRF on Postoperative Outcomes after Apicoectomy 81

5.2.3. Composite Use of A-PRF and BoneAlbumin in Bone Regeneration 85

5.3. Limitations 88

5.3.1. Limitations of the 3D Scanner Validation Study 88

5.3.2. Limitations of the Randomized Controlled Trial 89

5.3.3. Limitations of the Case Report (BoneAlbumin + A-PRF) 91

5.4. Future Directions 92

6. Conclusion 94

7. Summary 96

8. References 97

9. Bibliography of Candidate's Publication 116

9.1. Publications Directly Related to the Dissertation 116

9.2. Publications Not Related to the Dissertation 116

9.3. Total Cumulative Impact Factor 117

10. Acknowledgements 118

List of Abbreviations

3D	Three-Dimensional
A-PRF	Advanced Platelet-Rich Fibrin
BHA	Bovine-Derived Hydroxyapatite
CBCT	Cone Beam Computed Tomography
CSD	Critical Size Defect
DSLR	Digital Single-Lens Reflex
I-PRF	Injectable Platelet-Rich Fibrin
ICC	Intraclass Correlation Coefficient
IGF	Insulin-Like Growth Factor
ISQ	Implant Stability Quotient
L-PRF	Leukocyte- and Platelet-Rich Fibrin
MTA	Mineral Trioxide Aggregate
NB	Native Bone
NFB	Newly Formed Bone
NHP	Natural Head Position
NMT	Non-Mineralized Tissue

OKC	Odontogenic Keratocyst
PDGF	Platelet-Derived Growth Factor
PRF	Platelet-Rich Fibrin
PROMIS	Patient-Reported Outcomes Measurement Information System
QoL	Quality of Life
RG	Residual Graft
S-PRF	Standard Platelet-Rich Fibrin
SHA	Synthetic Hydroxyapatite
SLR	Single-Lens Reflex
SPSS	Statistical Package for the Social Sciences
STL	Standard Tessellation Language
TGF-β1	Transforming Growth Factor Beta 1
VAS	Visual Analog Scale
μCT	Microcomputed Tomography

1. Introduction

1.1.General Concepts of Wound Healing

Definition and Phases of Wound Healing

Wound healing is the physiological cascade through which damaged tissues re-establish structural integrity and functional capacity.[1] In the context of oral and maxillofacial surgery, this process encompasses the repair of highly vascularized mucosa, mineralized bone, and connective tissue—each with distinct biological characteristics and temporal dynamics.[2,3]

The healing response is conventionally divided into four interdependent and overlapping phases:

Hemostasis – Platelet aggregation and fibrin clot formation occur immediately after injury, limiting hemorrhage and initiating molecular signaling.[4]

Inflammation – Neutrophils and macrophages infiltrate the site to remove necrotic material and secrete cytokines and growth factors that coordinate the downstream healing cascade.[5,6]

Proliferation – Cellular proliferation and extracellular matrix deposition are driven by fibroblasts, endothelial cells, and keratinocytes, promoting angiogenesis and granulation tissue formation.[1,4]

Remodeling – Collagen fiber alignment, matrix turnover, and eventual revascularization lead to structural stabilization and functional tissue maturation.[1]

Intraoral wounds typically exhibit accelerated healing compared to cutaneous wounds, owing to enhanced perfusion, saliva-mediated biochemical support, and a modulated local immune environment.[1,7] The distinctive characteristics of the

oral environment justify the use of biologically active materials such as platelet-rich fibrin (PRF), which can influence multiple phases of wound healing and potentially enhance surgical results.[2,8]

1.2. PRF and its Role in Regenerative Surgery

1.2.1. Platelet Rich Fibrin (PRF)

The concept of platelet-rich preparations dates back to the 1950s, when Kingsley first used the term “platelet-rich plasma” (PRP) to describe thrombocyte concentrates administered to patients with thrombocytopenia. [9] In the following decades, particularly during the 1970s, the term became more widely adopted in hematology, and various protocols were developed for the preparation and clinical use of PRP.[8,10] Early techniques often relied on the addition of anticoagulants to prevent premature coagulation and maintain the concentrate in a liquid state.[8,11] These methods, however, were frequently time-consuming and yielded inconsistent outcomes. Parallel to these developments,[10] Matras conducted experimental studies on skin wound healing in rats, introducing the use of “fibrin glue” as a potential enhancer of tissue regeneration.[12] Platelet concentrates began to gain traction across various surgical disciplines, including neurosurgery and ophthalmology.[13] A pivotal moment in the context of oral and maxillofacial surgery came in 1998, when Marx et al. demonstrated that autologous platelet-enriched plasma significantly improved the rate and quality of bone regeneration in grafting procedures, sparking increased interest in platelet-based regenerative approaches within the field.[14]

In response to the limitations associated with first-generation platelet concentrates, a second-generation product platelet-rich fibrin (PRF) was introduced by Choukroun and colleagues in 2000.[15] Unlike PRP, the preparation of PRF does not require the addition of anticoagulants or exogenous thrombin.[16] Instead, it involves the immediate centrifugation of freshly drawn venous blood, allowing for a natural coagulation process that results in a firm, fibrin-rich matrix.[17] This simplified

protocol yields a more physiologically stable biomaterial, in which leukocytes and platelets are embedded within a three-dimensional fibrin scaffold.[2,3] The structural integrity of PRF not only enables sustained release of growth factors over an extended period, but also enhances mechanical handling properties during surgical application.[8,18] The introduction of PRF marked a conceptual shift in the use of autologous blood derivatives, emphasizing biological compatibility, ease of preparation, and improved regenerative performance, particularly in the context of soft and hard tissue healing in oral and maxillofacial surgery.[18,19]

1.2.2. Biological Mechanism of Action

The clinical interest in platelet-rich fibrin (PRF) stems from its ability to modulate key biological processes involved in wound healing and tissue regeneration. As a leukocyte- and platelet-rich autologous biomaterial embedded in a fibrin scaffold, PRF acts not merely as a passive filler, but as a biologically active matrix capable of orchestrating a wide range of cellular and molecular events.[2]

Platelets are anuclear cell fragments derived from bone marrow megakaryocytes, with a typical lifespan of 8–10 days. Their cytoplasm contains alpha and dense granules, which store various bioactive molecules. Alpha granules release proteins such as fibronectin, fibrinogen, and multiple growth factors, while dense granules contain calcium and serotonin. The platelet membrane includes receptors for molecules like collagen and thrombin, enabling activation at injury sites.[20,21]

Upon activation, platelets aggregate and contribute to hemostasis. Simultaneously, degranulation initiates the release of cytokines that promote cell migration and proliferation within the fibrin matrix, marking the onset of tissue repair.[21]

Fibrin Matrix in PRF:

The fibrin matrix forms the structural and biological foundation of PRF[16]. It results from the physiological conversion of fibrinogen to fibrin during

centrifugation, without the use of anticoagulants.[8] This process yields a dense, three-dimensional scaffold that entraps platelets and leukocytes, supporting their gradual release of bioactive molecules.[22] The slow polymerization of fibrin produces a stable clot with favorable porosity, mechanical strength, and biological activity facilitating cell migration, angiogenesis, and matrix remodeling. As such, the fibrin architecture is not merely a carrier, but an active participant in the regenerative effects of PRF.[16,22]

Platelet cytokines:

Transforming Growth Factor Beta-1 (TGF-β1)

TGF-β1 is the most abundantly secreted isoform of the TGF-β superfamily and plays a central role in wound healing through its profibrotic activity. Stored in platelet α-granules, it is released upon activation and regulates extracellular matrix production by stimulating the synthesis of collagen I and fibronectin, particularly in osteoblasts and fibroblasts. Although its effects on cell proliferation are context-dependent, TGF-β1 consistently promotes fibrous tissue formation and is therefore considered a key modulator of inflammation and early tissue remodeling.[23-25]

Platelet-Derived Growth Factors (PDGFs)

PDGFs are key mediators of wound healing that primarily regulate the migration, proliferation, and survival of mesenchymal cell lineages. Through interactions with specific receptors, they modulate cellular responses critical to tissue remodeling. Their regulatory role extends beyond repair, influencing embryonic development and contributing to fibroproliferative processes such as fibrosis and neoplasia. In the context of postoperative healing, PDGFs support connective tissue regeneration by orchestrating early cellular recruitment and matrix synthesis.[26-28]

Insulin-Like Growth Factors (IGFs)

IGF-I and IGF-II are potent regulators of cellular proliferation and differentiation across a wide range of cell types. Beyond their mitogenic activity, they play a pivotal anti-apoptotic role by transmitting survival signals that counteract extracellular matrix-induced cell death. Although IGFs are released during platelet degranulation, they are also abundantly present in systemic circulation. Their dual function as promoters of tissue regeneration and protectors against programmed cell death highlights their relevance in postoperative healing environments.[29,30]

Vascular endothelial growth factor (VEGF)

Vascular endothelial growth factor (VEGF) is another key mediator released from platelets during PRF activation. It plays a pivotal role in angiogenesis by promoting endothelial cell proliferation, migration, and new capillary formation at the site of injury. These effects are essential in ensuring adequate oxygen and nutrient supply for regenerating tissues. In the context of oral and maxillofacial surgery, VEGF contributes to improved vascularization of soft and hard tissues, which is particularly beneficial in early wound healing and graft integration. The sustained release of VEGF from the fibrin matrix enhances this angiogenic response over time, distinguishing PRF from earlier platelet concentrates with shorter activity profiles.[31-33]

Cellular components and immunomodulatory effects:

In addition to its fibrin scaffold and growth factor content, PRF exerts significant biological effects through its cellular components, particularly leukocytes.[34] The inclusion of neutrophils, monocytes, and lymphocytes within the matrix contributes to local immune regulation and inflammation control. These cells play an active role

in supporting tissue regeneration by modulating the healing environment and releasing secondary cytokines and antimicrobial peptides. Their presence enhances the biological complexity of PRF, highlighting it as a bioactive matrix that coordinates structural, molecular, and cellular processes during wound healing.[3,17]

1.2.3. PRF variants

Since its initial development by Choukroun in 2000, platelet-rich fibrin (PRF) has evolved significantly and today encompasses a broad range of biologically active formulations used in regenerative medicine.[15] PRF is considered a second-generation autologous platelet concentrate and was developed to overcome some limitations associated with platelet-rich plasma (PRP), such as the need for anticoagulants and complex preparation protocols.[35] In contrast, PRF is derived through a simplified single-centrifugation process without the addition of biochemical agents, making it safer, more cost-effective, and clinically practical.[18]

As interest in PRF has grown, several modifications in centrifugation protocols and tube materials have been introduced, resulting in a variety of PRF derivatives. These variants are tailored to optimize biological performance for specific clinical applications.[35]

Advanced Platelet-Rich Fibrin (A-PRF / A-PRF+)

A-PRF represents a refinement of L-PRF, developed through reduced centrifugal speed and increased duration (e.g., 1500 rpm for 14 minutes). This low-speed centrifugation concept enables a more homogeneous distribution of leukocytes and platelets throughout the clot, enhancing the biological profile of the final product.[35,36]

A-PRF and its enhanced variant, A-PRF+, demonstrate higher concentrations of growth factors and increased cell density, with studies reporting improved wound healing and regeneration, particularly in bone and soft tissue applications. These membranes retain a looser and more porous fibrin structure, allowing better cellular infiltration and sustained cytokine release.[17,37]

Besides A-PRF, various other PRF derivatives have been developed to optimize specific biological and clinical properties. (**Figure 1.)**

Figure 1. A-PRF+ membranes after centrifugation

Leukocyte-Platelet Rich Fibrin (L-PRF)

L-PRF is the most extensively studied and clinically applied PRF variant, providing a leukocyte- and platelet-rich fibrin scaffold that supports wound healing and tissue regeneration.[38]

Injectable Platelet-Rich Fibrin (I-PRF)

Injectable platelet-rich fibrin (i-PRF) is a liquid PRF formulation that can be delivered directly into tissues or combined with grafting materials, promoting cell migration, regeneration, and wound healing in both hard and soft tissue applications.[39]

Titanium Platelet-Rich Fibrin (T-PRF)

Titanium-prepared platelet-rich fibrin (T-PRF) is generated using titanium tubes and is characterized by a denser, more stable fibrin matrix with prolonged resorption, making it particularly suitable for regenerative procedures requiring extended healing periods.[40]

Horizontal Platelet-Rich Fibrin (H-PRF)

Horizontal platelet-rich fibrin (H-PRF) is produced using horizontal centrifugation, resulting in a more homogeneous distribution of cellular components and growth factors, with promising regenerative and antimicrobial properties.[41]

Albumin-Rich Platelet-Rich Fibrin (Alb-PRF)

Albumin-rich platelet-rich fibrin (Alb-PRF) combines PRF with heat-denatured albumin to create a mechanically stable, slowly resorbing biomaterial that provides prolonged structural support and sustained release of bioactive factors during tissue regeneration.[41]

Concentrated Platelet-Rich Fibrin (C-PRF)

Concentrated platelet-rich fibrin (C-PRF) is a highly enriched PRF formulation containing increased levels of platelets, leukocytes, and growth factors, which may enhance regenerative potential and support accelerated tissue healing.[42,43]

Antibiotic-Loaded Platelet-Rich Fibrin (A-PRF/Drug-Enhanced PRF)

Antibiotic-enhanced PRF is a modified PRF formulation that incorporates antimicrobial agents, combining regenerative properties with localized infection control and sustained drug delivery.[44]

1.2.4. Clinical Relevance in Oral and Maxillofacial Surgery

The use of platelet-rich fibrin (PRF) in oral and maxillofacial surgery has gained increasing clinical interest due to its autologous nature, ease of preparation, and regenerative potential across a range of surgical indications.[11] PRF supports wound healing through a combination of biological mechanisms sustained release of growth factors, leukocyte-mediated immune modulation, and the structural support of a dense fibrin matrix making it particularly well-suited for procedures involving both soft tissue and bone.[2,3,8]

The present work primarily focuses on the application of A-PRF in periapical surgery and its potential influence on postoperative pain, swelling, and patient quality of life, other reported clinical applications are reviewed only briefly for context.

Platelet-Rich Fibrin in Periapical Surgery:

In endodontic microsurgery, particularly apicoectomy, postoperative healing is often hindered by inflammation, swelling, and delayed bone regeneration.[45,46] Platelet-rich fibrin (PRF), as an autologous biomaterial rich in growth factors, has

gained attention for its potential to support both soft and hard tissue healing in these procedures.[47] By providing a biologically active scaffold, PRF may help modulate inflammation, enhance angiogenesis, and accelerate recovery.[17]

Clinical observations suggest that the use of PRF in periapical surgery can reduce postoperative discomfort and support more favorable healing trajectories.[48] Improvements in pain management, facial swelling, and patient-reported quality of life have been noted, alongside promising but variable radiographic bone healing outcomes.[48-50]

Platelet-Rich Fibrin and Its Impact on Pain, Swelling and Quality of Life:

In addition to its regenerative and anti-inflammatory properties, platelet-rich fibrin (PRF) has shown increasing potential in improving patient comfort and quality of life after surgical procedures.[51] A growing number of clinical studies and systematic reviews have examined PRF's influence on postoperative outcomes, particularly regarding pain perception, swelling, and functional recovery.[51-53]

Evidence suggests that PRF may reduce the intensity and variability of postoperative pain in various interventions, including third molar extractions, mucogingival surgery, periapical procedures, and soft tissue grafting.[53,54] In many of these cases, PRF use has also been associated with decreased analgesic consumption and lower swelling. While the precise mechanisms remain under investigation, the sustained release of growth factors and cytokines from PRF likely contributes to its pain-modulating effect and accelerated healing response.[51,55,56]

Furthermore, studies evaluating quality-of-life outcomes have reported benefits in domains such as sleep, speech, and physical function, particularly following endodontic surgery. Though differences in pain perception are not always

statistically significant, trends consistently favor PRF-treated patients in terms of subjective comfort and faster recovery.[54]

Overall, the integration of PRF appears to support not only tissue regeneration but also enhanced patient-centered outcomes, which are increasingly recognized as key indicators of clinical success. However, continued research with standardized protocols is needed to confirm these effects and define their scope across different procedures.[51]

Platelet-Rich Fibrin in Bone Grafting:

One of the most important applications of PRF in oral and maxillofacial surgery is bone grafting, where it may serve as an autologous adjunct or alternative to conventional graft materials, supporting bone regeneration while avoiding donor site morbidity.[57]

When combined with particulate bone grafts, PRF can be used to create so-called "sticky bone," improving graft handling and stability while supporting vascularization and bone regeneration.[58]

PRF has been successfully applied in alveolar ridge preservation, sinus augmentation, and peri-implant bone grafting, where it may enhance bone regeneration and support favorable clinical outcomes.[59-61]

Platelet-Rich Fibrin in Exodontia and Alveolar Healing:

PRF has been widely investigated in extraction socket management and alveolar ridge preservation. Through the sustained release of growth factors and the provision of a biologically active fibrin scaffold, PRF may enhance post-extraction

wound healing, promote bone formation, and help maintain alveolar ridge dimensions. Clinical studies have also reported reduced postoperative complications, including pain and alveolar osteitis, as well as improved conditions for subsequent implant placement.[56,62,63]

Platelet-Rich Fibrin in Sinus Augmentation Surgery:

PRF has also been applied in sinus augmentation procedures, where it may enhance bone regeneration and support graft maturation within the elevated sinus cavity. When combined with bone graft materials, PRF has been associated with improved healing and may shorten the time required before implant placement. Additionally, PRF membranes can be used in the management of Schneiderian membrane perforations, providing both mechanical support and biological stimulation during healing.[59,64,65]

Platelet-Rich Fibrin in Periodontal Healing:

PRF has become an important adjunct in periodontal regenerative procedures, demonstrating beneficial effects on soft tissue healing, clinical attachment gain, and regeneration of intrabony defects. Beyond periodontal defect management, PRF has also been successfully applied in mucogingival surgery and other regenerative procedures, highlighting its broad applicability in periodontal therapy.[66,67]

Platelet-Rich Fibrin in Surgical Management of Bone Cysts:

PRF has also been investigated in the management of cystic bone defects of the jaws, where it may promote bone healing and soft tissue regeneration following cyst enucleation. Used alone or in combination with bone graft materials, PRF has

shown promising results in enhancing defect fill and supporting postoperative healing, although further high-quality studies are needed to confirm its long-term clinical benefits.[57,68,69] (**Figure 2.)**

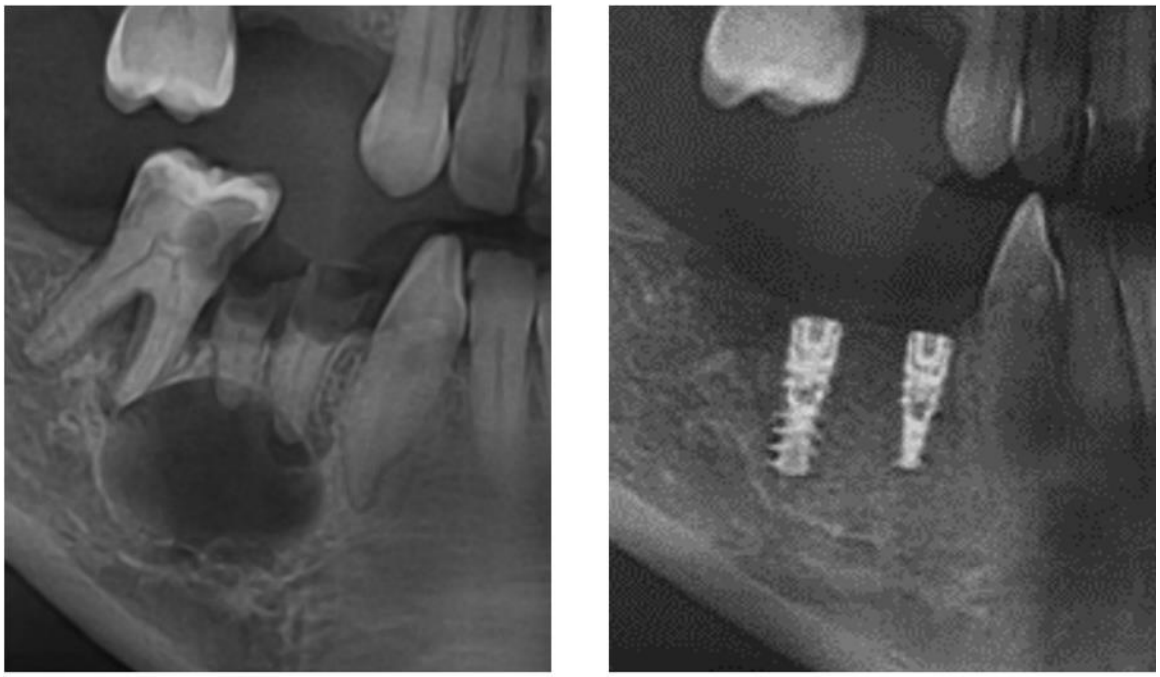

Figure 2. (**a**) Odontogenic bone cist in the mandible, (**b**) The lesion is completly healed after augmentation with sticky bone, and after 3 months implants were placed in the augmented area.

Platelet-Rich Fibrin in Oroantral Communications Closure:

PRF has been used in the management of oroantral communications (OAC), either alone or in combination with conventional closure techniques. Its biologically active fibrin matrix may support soft tissue healing, enhance wound stability, and promote mucosal regeneration, making it a promising adjunct in the treatment of complex or recurrent defects.[70,71]

Platelet-Rich Fibrin in Soft Tissue Grafting:

PRF has gained increasing attention in soft tissue grafting and mucogingival surgery due to its ability to promote wound healing and tissue regeneration through the sustained release of growth factors. Applied alone or in combination with connective tissue grafts, PRF has been associated with favorable healing outcomes, reduced postoperative discomfort, and improved soft tissue management around teeth and implants.[72,73]

Platelet-Rich Fibrin in Cleft Patient Reconstruction:

Platelet-rich fibrin (PRF) has been explored as a supportive adjunct in alveolar cleft reconstruction. When combined with autogenous bone grafts, PRF may enhance bone regeneration by providing a concentrated source of bioactive molecules. Clinical comparisons have indicated that PRF use can lead to increased new bone formation in cleft sites, suggesting potential benefits in graft integration and healing outcomes.[47,63,74]

Platelet-Rich Fibrin in the Management of Medication-Related Osteonecrosis of the Jaw (MRONJ):

The management of medication-related osteonecrosis of the jaw (MRONJ) has recently incorporated PRF as a regenerative adjunct aimed at improving healing outcomes. Owing to its regenerative and anti-inflammatory properties, PRF may support soft and hard tissue healing following surgical debridement, with clinical studies reporting favorable outcomes in terms of pain reduction, wound healing, and overall recovery. Although further evidence is required, PRF represents a biologically supportive approach in MRONJ treatment.[75-77]

Platelet-Rich Fibrin in Endodontics:

Regenerative endodontic procedures (REPs) have increasingly incorporated PRF as a biologically active scaffold capable of supporting tissue repair and root development in immature teeth with necrotic pulp. Through its sustained release of growth factors and support of cellular migration and differentiation, PRF has been associated with improved periapical healing and favorable regenerative outcomes, making it a promising adjunct in regenerative endodontic therapy.[50,78]

Platelet-Rich Fibrin in Dental Implantology: Enhancing Osseointegration and Healing:

Implant dentistry represents another important field of PRF application. Owing to its regenerative properties, PRF has been used to support osseointegration, enhance soft and hard tissue healing, and improve outcomes in procedures such as ridge preservation and bone augmentation. Although further high-quality evidence is needed, current studies suggest a beneficial effect of PRF on early implant healing and stability.[72,79,80]

Platelet-Rich Fibrin in the Management of Peri-Implantitis:

Platelet concentrates (PCs), including platelet-rich fibrin (PRF), have gained increasing attention as adjunctive therapies in the management of peri-implantitis (PI). Current evidence suggests that PRF may support soft and hard tissue healing around compromised implants and improve clinical parameters such as probing depth, bleeding on probing, and marginal bone stability. However, further standardized clinical studies are required to establish its definitive role in PI treatment.[39,61]

Platelet-Rich Fibrin in Temporomandibular Joint Disorders:

Injectable platelet-rich fibrin (i-PRF) has shown promising results in the management of temporomandibular joint (TMJ) disorders. Clinical studies suggest that intra-articular i-PRF injections may reduce pain and improve joint function, potentially supporting tissue regeneration and inflammation control. Nevertheless, further high-quality studies are needed to confirm its long-term efficacy.[43,81]

1.3. 3D Facial Scanning in Oral and Maxillofacial Surgery

Three-dimensional (3D) facial scanning technology has become increasingly utilized across various domains such as healthcare, security, and digital media. In clinical and research settings, its primary applications include precise individual identification, enhancement of diagnostic accuracy, and the facilitation of detailed anatomical analysis within virtual environments.[82,83] (**Figure 3**.)

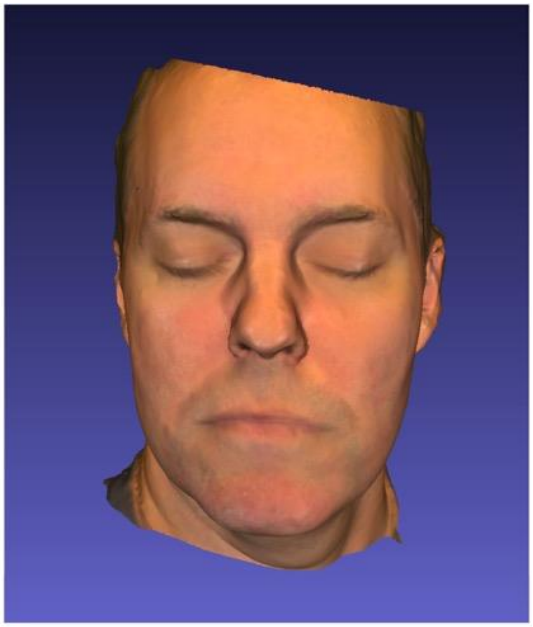

Figure 3. 3D facial scan

Three-dimensional (3D) facial imaging systems represent powerful tools for comprehensive facial assessment, offering significant utility in both clinical and research contexts. Their applications include preoperative planning, postoperative evaluation of facial symmetry, and the assessment of surgical morphological changes. Moreover, their integration into forensic medicine supports precise documentation and analysis. The strong correlation between skeletal and soft tissue structures further enhances their relevance in maxillofacial diagnostics and treatment planning.[84,85] Soft tissue facial anthropometry plays a critical role in clinical practice by providing objective and quantifiable data on craniofacial development, which serves as a fundamental basis for both surgical planning and the evaluation of therapeutic outcomes.[86] Three-dimensional imaging systems also contribute to the accurate diagnosis of craniofacial syndromes through the assessment of both normal and pathological growth patterns, thereby supporting surgical planning in maxillofacial procedures and informing orthodontic interventions. In cases such as cleft lip, the evaluation of facial appearance relies on a combination of direct clinical anthropometry, two- and three-dimensional imaging modalities, as well as clinical videography, enabling both qualitative and quantitative analysis of the oro-maxillofacial region.[87-89]

Three-dimensional facial recognition has become a key technology in the fields of security and identity verification, surpassing traditional two-dimensional methods in accuracy and reliability. As a major application of 3D facial scanning, this approach has been the focus of extensive research. The literature highlights the development of techniques capable of handling challenges such as variations in facial expression, head position, lighting conditions, and partial occlusions. Recent advancements in 3D imaging and machine learning have further improved the robustness and applicability of facial recognition systems across diverse environments.[90-92]

Recent advances in 3D imaging have significantly expanded its utility, ranging from access control systems to clinical and forensic applications. In forensic medicine, accurate documentation of traumatic injuries is essential for both legal and

diagnostic purposes. Structured light and LiDAR-based 3D scanning technologies offer enhanced precision and reproducibility, enabling detailed surface mapping that surpasses the limitations of traditional photography. These capabilities make 3D scanning a valuable tool in forensic pathology, particularly for documenting injury patterns and post-mortem findings in a standardized and objective manner.[92,93]

In recent decades, significant technological advancements have led to a shift from traditional direct anthropometry typically performed with rulers and calipers and two-dimensional (2D) photography toward non-invasive three-dimensional (3D) surface imaging techniques. While direct caliper-based measurement remains a straightforward and low-cost method, it is limited by its dependency on physical contact and examiner experience. Similarly, although 2D imaging is cost-effective, it requires substantial patient cooperation and often lacks the precision needed to detect subtle craniofacial asymmetries or disproportions.[94,95]

Multiple imaging modalities have been developed for visualizing facial soft tissues, including ultrasound, laser scanning, and soft-tissue reconstructions from computed tomography (CT) data. However, among these, digital stereophotogrammetry is widely regarded as the most reliable technique, owing to its superior accuracy, processing speed, and overall reproducibility. Currently, digital stereophotogrammetry represents one of the most widely adopted methods for capturing three-dimensional images of the facial surface.[96-98] This method captures the facial surface using multiple synchronized digital SLR cameras with overlapping fields of view, allowing the reconstruction of a comprehensive three-dimensional model through specialized software. The resulting geometry is rendered as a dense point cloud with realistic skin texture. Owing to its accuracy and non-invasive nature, stereophotogrammetry is considered one of the most reliable techniques for soft-tissue analysis. The generated 3D models enable precise measurements of various morphological parameters, including distances, angles, curvatures, volumes, and surface areas. Furthermore, the ability to view the face from any angle enhances its utility, while the speed of data acquisition surpasses

that of conventional clinical photography. Unlike direct anthropometry, measurements can be performed retrospectively without requiring the patient's presence, minimizing errors related to soft tissue distortion.[99-102]

Three-dimensional (3D) imaging with digital light scanners has become increasingly prevalent in medical applications, largely due to improvements in accessibility and affordability. These scanners enable the acquisition of detailed surface morphology, which can be processed and analyzed using standard computer software. Operating by capturing reflected light, these devices generate depth and texture data of facial structures. While they offer distinct advantages such as non-invasive data collection, ease of use, and patient comfort they also present certain limitations, including variability in accuracy, data acquisition time, and processing requirements. As 3D facial data are increasingly used in surgical planning and clinical evaluation, ensuring the precision and reliability of these devices is essential. High measurement accuracy remains a prerequisite for integrating 3D scanning technology into clinical workflows.[103-105]

Although the reliability of various facial measurement methods has been well-documented, further investigation is required regarding scanning duration, data processing workflows, and overall measurement consistency. The rapid development of scanning technologies and the emergence of newer surface scanners have improved the accessibility of 3D surface imaging. Nonetheless, before these systems can be fully integrated into clinical practice, their accuracy and reproducibility must be established through rigorous validation studies.[82]

2. Objectives

The primary objective of this dissertation was to evaluate the effects of platelet-rich fibrin (PRF) on postoperative healing and tissue regeneration following oral and maxillofacial surgical procedures. Particular emphasis was placed on patient-centered outcomes after periapical surgery, including postoperative pain, facial swelling, and oral health-related quality of life.

Additional observations regarding the regenerative potential of PRF were obtained from selected clinical applications involving bone healing and augmentation, using radiological and histological evaluation methods.

To facilitate objective assessment of postoperative swelling, a three-dimensional structured-light facial scanner (EINSTAR, Shining 3D, China) was validated and applied as a quantitative measurement tool during clinical follow-up.

It was hypothesized that the application of autologous PRF would improve postoperative healing and regenerative outcomes compared with conventional treatment alone. Specifically, PRF was expected to reduce postoperative pain and facial swelling, improve patient-reported quality of life, and promote tissue regeneration. Furthermore, three-dimensional facial scanning was expected to provide a reliable and reproducible method for the objective assessment of postoperative swelling.

3. Methods

This dissertation is based on three interrelated investigations, all focusing on the clinical applications and regenerative potential of platelet-rich fibrin (PRF) in oral and maxillofacial surgery. The studies were conducted independently but aligned around a shared aim of evaluating PRF's effect on healing dynamics and patient-centered outcomes. In addition, the clinical validation and implementation of a non-invasive, three-dimensional facial scanning system was performed to provide objective and reproducible soft tissue measurements during postoperative follow-up.

To ensure scientific transparency and methodological reproducibility, each study is described in detail in the subsections below, covering patient selection, clinical protocols, biomaterial preparation, imaging methodology, data acquisition, and statistical analysis.

The three main research components were:

- Validation of a 3D Facial Scanner for Craniofacial Anthropometry
- Randomized Controlled Clinical Trial: The Effect of PRF on Postoperative Outcomes after Apicoectomy
- Case Report: Composite Use of A-PRF and Albumin-Coated Allograft in a Patient with Gorlin–Goltz Syndrome

3.1. Validation of a 3D Facial Scanner for Craniofacial Anthropometry

3.1.1. Study Participants

A total of eleven healthy volunteers were recruited for the present validation study, including six females and five males, with an age range of 18 to 58 years (mean age: 31 years). The sample size was determined based on the design and outcomes of a previously published validation study by Basier Ngueira et al., in which a similar participant number yielded clinically relevant results. Their findings demonstrated that a 3D photogrammetric scanning system achieved high intra- and inter-examiner reliability (intraclass correlation coefficient [ICC] > 0.9) and minimal measurement variation, with a mean difference of −0.8 ± 1.2 mm compared to digital caliper values.[106]

Inclusion criteria required the absence of any conditions that could interfere with normal facial anatomy. Accordingly, subjects with a history of previous unilateral or bilateral facial surgery, trauma, congenital deformities, or any facial intervention that could alter the soft tissue contours were excluded from participation.

All participants provided written informed consent prior to enrollment, authorizing the use of their facial images and anonymized data for research and publication purposes. The study protocol was reviewed and approved by the Institutional Ethics Committee of Semmelweis University (reference number: SE RKEB: 265/2019).

3.1.2. Examiners

Two independent examiners participated in the measurement process. The first examiner had prior experience in both digital facial scanning and cephalometric analysis, while the second examiner had no previous training in these techniques. In order to ensure consistency, the identification and marking of anatomical facial landmarks were jointly performed by both examiners before any measurements were taken. Following landmark placement, each examiner independently

conducted direct anthropometric measurements using a digital caliper on the live subjects. Subsequently, three-dimensional facial scans were obtained, and indirect measurements were performed on the resulting digital models by both examiners.

3.1.3. Three-Dimensional Imaging and Measurement Protocol

Prior to data acquisition, all participants were instructed to remove jewelry and ensure that hair was cleared from the facial and forehead regions to provide unobstructed access to the areas of interest. Male participants were additionally asked to shave any facial hair to avoid interference with scanning accuracy.

Fourteen anatomical cephalometric landmarks were defined for the purposes of the study, based on established protocols and selected using the mirror application (Canfield Scientific, Parsippany, NJ, USA).[107] In total, eleven linear measurements were obtained, encompassing horizontal, vertical, and oblique dimensions. The selection of reference points was informed by prior literature, ensuring the inclusion of clinically relevant anatomical locations while allowing for methodological consistency with analogous studies. To enhance measurement precision, the selected landmarks were pre-marked using a sterile Devon skin marker (Covidien Inc., Minato City, Japan), as this has been demonstrated to reduce measurement variability. The chosen landmarks and distances aimed to capture a representative spatial distribution across the face, facilitating a comprehensive evaluation of the scanner's dimensional accuracy and potential directional distortion.[94]

The anatomical reference points selected for this study represent widely accepted cephalometric landmarks relevant for soft tissue analysis. These landmarks were defined to ensure comprehensive spatial coverage of the facial anatomy and to enable the assessment of dimensional accuracy across multiple facial planes. The following soft tissue points were used: **(Figure 4.)**

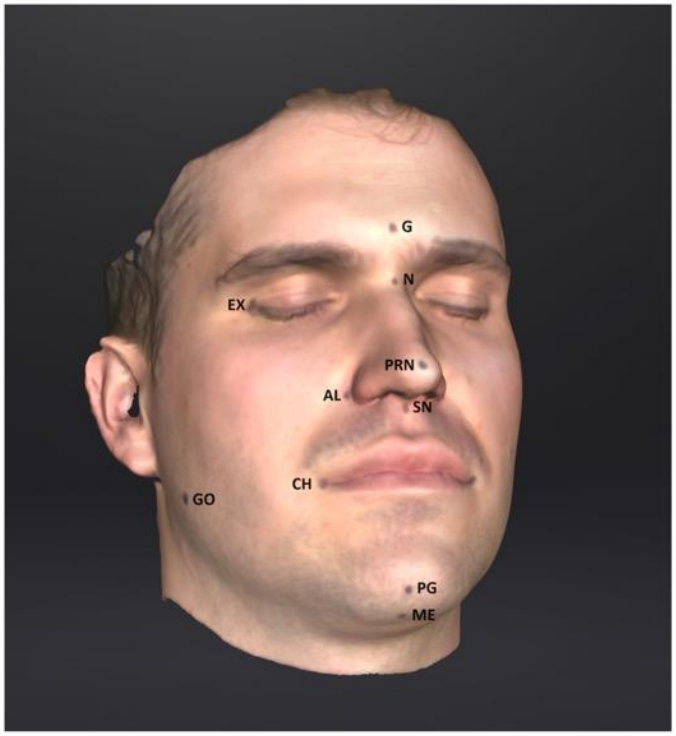

Figure 4. The cephalometric reference points.

- **Glabella (G):** The most anterior midpoint on the fronto-orbital contour.
- **Nasion (N):** The midpoint at the base of the nasal root, corresponding to the frontonasal suture.
- **Subnasale (Sn):** The midpoint of the nasolabial contour, located between the columella crest and the upper lip.
- **Pronasale (Prn):** The most anterior point on the nasal tip.
- **Alare right and left (Alr, All):** The most lateral points on the respective right and left alar contours.
- **Pogonion (Pg):** The most anterior midpoint of the soft tissue chin.
- **Menton (Me):** The most inferior midpoint on the chin's soft tissue contour.
- **Chelion right and left (Chr, Chl):** The points at the right and left labial commissures.
- **Exocanthion right and left (Exr, Exl):** The outer commissures of the right and left eye fissures.

- **Gonion right and left (Gor, Gol):** The most lateral points of the mandibular angles.

Based on these reference points, the following eleven linear measurements were obtained to evaluate facial dimensions in horizontal, vertical, and oblique directions:

- Glabella–Subnasale
- Subnasale–Menton
- Nasion–Pronasale
- Subnasale–Pronasale
- Exocanthion Right–Exocanthion Left
- Chelion Right–Chelion Left
- Exocanthion Right–Chelion Right
- Exocanthion Left–Chelion Left
- Gonion Right–Pogonion
- Gonion Left–Pogonion
- Alare Right–Alare Left

These measurements were selected to capture a range of clinically relevant facial distances, enabling assessment of both scanner accuracy and the influence of examiner experience across different anatomical regions.

During all measurement procedures, participants were seated in an upright position, maintaining a natural head posture with eyes gently closed, facial muscles relaxed, and without any active facial expression. This standardized positioning was essential to minimize soft tissue distortion and ensure repeatability.

Direct anthropometric measurements were performed using a precision digital caliper (Silverline, Iddesleigh, UK) with an accuracy of 0.01 mm. The caliper tips were gently placed on the previously marked cephalometric landmarks, taking care not to apply pressure that could deform the soft tissue surface.

For three-dimensional facial imaging, the EINSTAR structured light scanner (Shining 3D, Hangzhou, China) was employed. (**Figure 5.)** This portable scanner utilizes structured light technology to capture high-resolution surface data. The scanning procedure was conducted under consistent ambient lighting conditions, and subjects were instructed to remain still during image acquisition to prevent motion artifacts. The following settings were used for scanning:

- **Scan mode:** Portrait scan
- **Alignment:** Hybrid
- **Resolution:** 0.2 mm
- **Data Quality Indicator:** On
- **Hair mode:** Off

Figure 5. The EINSTAR scanner and accessories

Scanning procedures were conducted under natural ambient light to ensure consistent illumination and minimize artifacts. Post-processing of the acquired 3D facial data and subsequent indirect measurements were performed using the manufacturer's proprietary software, ExStar (v1.2). The EINSTAR scanner required connection to a Microsoft Windows-based personal computer throughout the scanning and processing workflow. The following system specifications were recommended to ensure optimal performance:

- **Operating system:** Windows 10 or 11 (64-bit)
- **Graphics card:** NVIDIA GTX1060 or higher
- **Video memory:** ≥6 GB
- **Processor:** Intel Core i7-11800H
- **System memory (RAM):** ≥32 GB

3.1.4. Time Analysis

To assess the time efficiency of the two measurement methods, the duration of each procedure was recorded using a digital stopwatch (ACCUSPLIT Pro Survivor—A601X, Torrance, CA, USA). For the conventional direct measurement method using a caliper, a single continuous time interval was measured per participant. In contrast, the workflow involving the 3D scanner was segmented into three distinct time intervals: (1) the scanning phase, during which the 3D facial surface was captured; (2) the post-processing phase, where the acquired data were reconstructed and refined using the proprietary ExStar software; and (3) the indirect measurement phase, in which the predefined linear distances were extracted from the finalized digital facial model. This structured timing approach allowed for a detailed comparison of the temporal requirements associated with each method, offering insight into their respective efficiencies in clinical and research contexts.

3.1.5. Statistical Analysis

Statistical analysis were performed using IBM SPSS Statistics software (version 25, IBM Corp., Armonk, NY, USA). The Kolmogorov–Smirnov test was applied to assess the normality of the data distribution. A 95% confidence interval was established, and statistical significance was defined at a p-value of less than 0.05.

To compare paired measurements obtained from the same subjects, paired-samples t-tests were used when the assumption of normality was met. The association between different sets of measurements was evaluated using Spearman's rank correlation coefficient, while measurement reliability was assessed using the intraclass correlation coefficient (ICC).

A structured overview of the research process is presented in the following flowchart to illustrate the methodological sequence and data collection workflow. (**Figure 6.**)

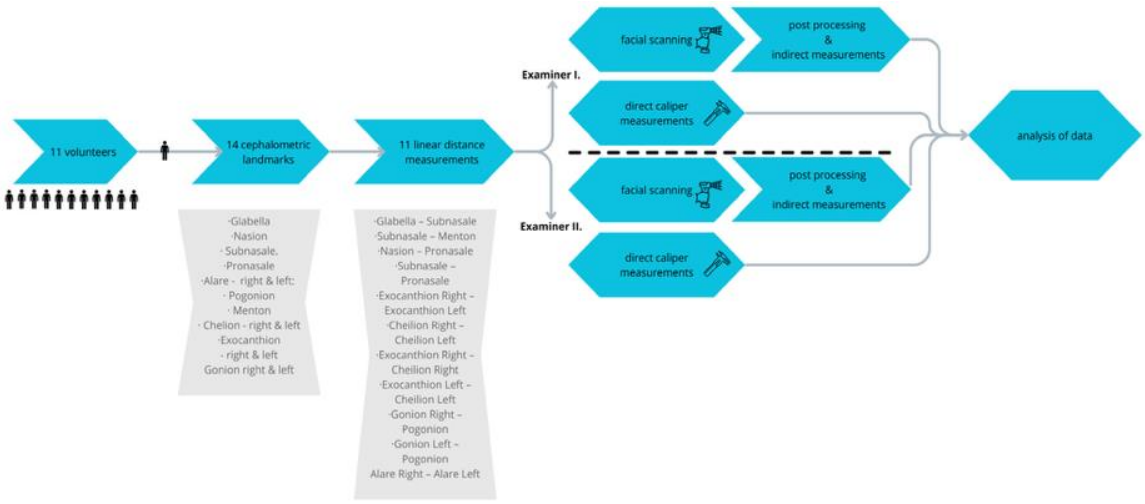

Figure 6. Steps and processes involved in the research.

3.2. Randomized Controlled Clinical Trial: The Effect of PRF on Postoperative Outcomes after Apicoectomy

3.2.1. Study Design

This prospective, preliminary randomized controlled clinical trial was designed to assess the efficacy of platelet-rich fibrin (PRF) membranes in promoting postoperative recovery following periapical surgery (apicoectomy). The research was conducted at the Department of Oro-Maxillofacial Surgery and Stomatology, Semmelweis University. The primary objective was to investigate whether the intraoperative application of autologous PRF membranes could reduce postoperative swelling and pain, and improve overall patient-reported outcomes. The trial followed a parallel-group design with two arms (intervention vs. control), and was carried out in accordance with ethical guidelines and institutional standards for clinical research.

3.2.2. Participants

A total of twenty patients were enrolled in this randomized controlled clinical trial and were allocated into two equal groups (1:1 ratio). All procedures were performed at the Department of Oro-Maxillofacial Surgery and Stomatology, Semmelweis University, by the same experienced surgeon to ensure procedural standardization.

- **PRF Group (n = 10):**

  Patients underwent a standard apicoectomy procedure complemented by the application of autologous platelet-rich fibrin (PRF) membranes. The PRF was positioned over the resected root-end and placed within the osteotomy site prior to flap closure.

- **Control Group (n = 10):**

  Patients received the standard apicoectomy procedure without PRF membranes. Only the routine root-end filling material was used, identical in both groups.

  Postoperative recovery was assessed using a multimodal evaluation framework designed to capture both objective and subjective outcomes. Facial swelling was quantified using standardized three-dimensional facial scanning, providing precise volumetric data on soft tissue changes. Pain intensity was monitored on a daily basis with the aid of a visual analog scale (VAS), allowing for consistent tracking of discomfort over time. In addition, health-related quality of life was evaluated using the PROMIS-29+2 Profile v2.1 questionnaire, which encompasses multiple patient-reported outcome domains relevant to postoperative recovery.[66,108]

3.2.3. Eligibility Criteria

Participants were eligible for inclusion if they were between 20 and 65 years of age, regardless of sex, and required an apicoectomy of maxillary or mandibular anterior or premolar teeth (from second premolar to second premolar) due to persistent periapical pathology. Indications included chronic apical periodontitis, symptomatic periapical lesions, or radiographically visible periapical radiolucencies accompanied by clinical signs such as percussion sensitivity, localized swelling, or the presence of a sinus tract. Final diagnosis was based on both clinical examination and periapical radiographs.

Exclusion criteria comprised the presence of systemic diseases such as uncontrolled diabetes mellitus, neuropsychiatric disorders, immunosuppressive conditions, the use of anticoagulant or immunosuppressive therapy, pregnancy or lactation, and any absolute contraindication to oral surgical procedures. These criteria were established to ensure a medically stable and homogeneous study population.

Routine hematological testing, including platelet counts, was not performed, as all participants were classified as ASA I–II and reported no history of hematologic disorders, bleeding tendencies, or medications known to influence platelet function.

3.2.4. Ethical Approval and Consent

The study protocol was reviewed and approved by the National Public Health Centre (Nemzeti Népegészségügyi Központ, NNK; registration number: 3736-1/2022/EKU), with official approval granted on 17 January 2023. All procedures involving human participants were carried out in full compliance with the ethical principles outlined in the Declaration of Helsinki (2024 revision) and its subsequent amendments, as well as other relevant national and institutional ethical standards.

3.2.5. Trial Registration and Informed Consent

This clinical trial was registered on the international database ClinicalTrials.gov (Identifier: NCT06739200), with the initial posting date on 18 December 2024. Registration ensured transparency, adherence to international standards, and public accessibility of the study protocol.

Prior to initiating any study-related procedures, written informed consent was obtained from all participants. Each subject received detailed verbal and written information regarding the study's purpose, methodology, potential risks, and anticipated benefits. Participants also gave explicit written consent for the anonymized use of data and facial images for research and publication purposes. The consent process adhered strictly to contemporary ethical guidelines, ensuring participant autonomy and data protection.

3.2.6. Randomization and Allocation Concealment

Participants were randomly assigned to the PRF and control groups in a 1:1 allocation ratio. The randomization sequence was generated using the random number generator function of IBM SPSS Statistics (version 26; IBM Corp., Armonk, NY, USA) by an independent research coordinator at Semmelweis University, who was not involved in participant recruitment, surgical procedures, or outcome evaluation.

To ensure proper allocation concealment, sequentially numbered, opaque, sealed envelopes (SNOSE) were prepared in accordance with the randomization list. At the time of surgery, the envelope corresponding to the participant's number was opened by a surgical assistant uninvolved in any part of the clinical assessment or data collection. This approach ensured strict concealment and minimized the risk of selection bias.

3.2.7. Blinding

This study was designed as a single-blind randomized controlled trial. Participants were blinded to group allocation throughout the study period. Outcome assessment was performed by independent evaluators who were likewise blinded to treatment allocation, thereby reducing the risk of detection bias.

Venous blood collection was performed exclusively in the PRF group, as obtaining blood samples from control participants without therapeutic justification would have been ethically inappropriate. Due to the procedural nature of the intervention, the operating surgeon could not be blinded. However, to mitigate potential performance and assessment bias, all postoperative outcome data including swelling, pain, and quality of life were collected and analyzed by assessors who remained unaware of group assignment.

3.2.8. Surgical Procedure

All surgical procedures were performed by the same experienced oral surgeon at the Department of Oro-Maxillofacial Surgery and Stomatology, Semmelweis University, in order to ensure standardization and procedural consistency across cases.

Local anesthesia was administered using 2% lidocaine with epinephrine. A trapezoidal submarginal flap was elevated following the Ochsenbein–Luebke design to access the affected periapical region.[109] Subsequently, 3 mm of the apical portion of the root was resected perpendicularly to its long axis. A retrograde cavity, 3 mm in depth, was prepared using ultrasonic surgical tips and filled with mineral trioxide aggregate (MTA), a widely validated material for root-end fillings.[110]

In the PRF group, platelet-rich fibrin membranes were prepared immediately prior to surgery according to the PRF Plus protocol (Process for PRF, Nice, France), in compliance with national venipuncture regulations (HarmonyCom, Hungary) and the manufacturer's recommendations. A 10 mL sample of autologous venous blood was collected from each patient into sterile, additive-free, plain glass tubes. Within one minute of collection, the samples were centrifuged using an IntraSpin® fixed-angle centrifuge (33° rotor angle; Intra-Lock International Europe, Salerno, Italy) at 1300 rpm for 8 minutes, equivalent to ~200 g of relative centrifugal force (RCF). The resultant fibrin clots were then compressed using a standardized PRF Box (Process for PRF) to produce membranes of uniform thickness.[8] These membranes were placed into the osteotomy cavity and over the resected root-end prior to flap closure.[111]

In the control group, the surgical protocol was identical, except that neither PRF nor placebo was applied. This design ensured that any observed differences in healing outcomes could be attributed to the use of PRF.

Flap repositioning and closure were carried out with tension-free 3–0 silk sutures using the continuous locking technique.[112] All patients received identical postoperative care instructions and medications to standardize post-surgical management across groups.

3.2.9. Postoperative Care

All participants received standardized postoperative instructions and care. Analgesia was provided with diclofenac (50 mg), administered twice daily for three days, as part of a uniform pain management protocol across both groups.[45] Patients were instructed to maintain oral hygiene using a 0.12% chlorhexidine mouthwash twice daily for one week. Sutures were removed on the seventh postoperative day.

Routine antibiotic prophylaxis was not employed; antibiotics were reserved exclusively for cases with clinical indications, such as signs of infection. However, during the study period, no such indications arose, and none of the participants required antibiotic therapy.[113]

Given that pain reduction was one of the hypothesized benefits of PRF application, all patients regardless of group assignment received the same analgesic regimen. This approach ensured that no participant remained untreated for postoperative discomfort, in accordance with the ethical principles outlined in the Declaration of Helsinki.

Although blinding of the operating surgeon was not feasible due to the nature of the intervention, measures were taken to minimize bias. These included patient blinding, blinded outcome assessment, and the implementation of a fully standardized postoperative care protocol.

3.2.10. Outcome Measures

Postoperative recovery was evaluated based on three primary outcome domains: health-related quality of life, pain intensity, and facial swelling. All outcomes were assessed using validated instruments at standardized time points to ensure consistency and reliability.

Quality of Life (QoL):

Health-related QoL was measured using the PROMIS-29+2 Profile v2.1 questionnaire. This validated tool evaluates multiple domains including physical function, emotional well-being, pain interference, fatigue, sleep disturbance, and social participation. Assessments were carried out preoperatively and again on postoperative day 7 to capture changes related to the surgical intervention and recovery process.[114]

Pain Intensity:

Postoperative pain was self-reported daily by participants using a 10-point visual analog scale (VAS) for seven consecutive days. On this scale, 0 represented no pain, while 10 indicated the worst imaginable pain.[115] This approach provided a continuous and patient-centered measure of discomfort across the early healing phase.

Facial Swelling:

Facial swelling was quantified using three-dimensional optical surface scans obtained with the Einstar 3D scanner(Shining 3D, Hangzhou, China). Scans were taken at two time points: preoperatively (T0) and on postoperative day 3 (T1).

The 3D datasets were digitally aligned, and volumetric changes were calculated using Boolean subtraction techniques to determine the precise extent of swelling based on soft tissue expansion.

3.2.11. Three-Dimensional Image Acquisition and Analysis

Three-dimensional (3D) facial surface images were obtained at two standardized time points: preoperatively (T0) and on postoperative day 3 (T1), using the **Einstar handheld extraoral 3D scanner** (Shining 3D, Hangzhou, China). This device has previously been validated for reliable and reproducible volumetric analysis of soft tissue in the craniofacial region.[82]

To ensure consistency during image acquisition, all participants were seated in the same dental chair, maintaining a natural head position (NHP) with relaxed facial muscles and closed eyes. Scanning was conducted following the manufacturer's standardized portrait scan protocol.

Initial post-processing of raw scan data was carried out using the scanner's ExStar software (v1.2), after which surface mesh files were exported in STL format for volumetric analysis. The preoperative and postoperative scans were aligned using a global best-fit algorithm in ZEISS GOM Inspect (v15.2; Zeiss, Oberkochen, Germany) to achieve optimal surface correspondence.

To refine the models and remove non-relevant areas, mesh trimming was performed in Meshmixer (Autodesk, San Francisco, CA, USA), following established methodology.[116] Trimming boundaries were defined based on anatomical planes: above the Frankfurt horizontal plane, below the hyoid bone, posterior to the preauricular skin crease, and posterior to the sternocleidomastoid muscle.

Volumetric changes were calculated by creating closed solid models from the trimmed surfaces and applying Boolean subtraction between the T1 and T0 scans.

This process yielded the absolute volume difference in cubic centimeters, representing the extent of postoperative facial swelling.

3.2.12. Statistical Analysis

Statistical analysis was performed using IBM SPSS Statistics (Version 25.0, IBM Corp., Armonk, NY, USA). A significance level of $\alpha = 0.05$ was applied, and all p-values were reported as two-tailed. Confidence intervals (95% CI) were calculated where appropriate to provide precise estimates.

3.2.12.1. Normality Testing

The distribution of each outcome variable was assessed using the Kolmogorov–Smirnov test to determine whether parametric or non-parametric statistical methods were appropriate. In cases where normal distribution was confirmed, independent-samples t-tests were applied to compare outcomes between the PRF and control groups, while paired-samples t-tests were used to evaluate within-group changes (e.g., pre- and postoperative values). For variables that did not meet the assumption of normality, non-parametric tests were used: the Mann–Whitney U test for between-group comparisons and the Wilcoxon signed-rank test for paired, within-group analyses. The choice of statistical tests was thus based on the distributional characteristics of each variable.

3.2.12.2. Between-Group Comparisons

Between-group differences in postoperative outcomes between the PRF and control groups were evaluated using parametric or non-parametric statistical methods, as appropriate, based on data distribution and variance homogeneity. The outcomes assessed included:

- **Volumetric facial swelling** (derived from 3D analysis),
- **Pain intensity** (measured via daily VAS scores),
- **Health-related quality of life domains** (assessed by the PROMIS-29+2 Profile v2.1).

Levene's test was used to assess the homogeneity of variances for each variable. Depending on the result, either equal or unequal variance models were applied when selecting the appropriate test statistics for each comparison.

3.2.12.3. Within-Group Comparisons

To assess the effect of the intervention within each group, pre- and postoperative differences were analyzed using paired-samples t-tests. This analysis focused primarily on:

- Changes in PROMIS-29+2 domain scores (e.g., physical function, sleep disturbance),
- Pain intensity scores as measured by the VAS.

These comparisons allowed for the evaluation of intra-group improvement or deterioration over the postoperative period.

3.2.12.4. Correlation Analysis

To investigate potential associations between the primary outcome variables, Pearson's correlation coefficients were calculated. The analysis focused on relationships between volumetric facial swelling (as measured via 3D scanning), pain intensity (VAS scores), and the various domains of the PROMIS-29+2 Profile v2.1 (e.g., physical function, pain interference). Correlation analyses were conducted both for the total sample and separately within each study group (PRF and control) to detect any group-specific trends or interactions.

3.2.12.5. Analytical Approach

A per-protocol analytical approach was applied in this study. All 20 participants completed the trial without any protocol deviations or dropouts, thereby allowing for consistent pairwise comparisons both within and between the PRF and control groups. Given the preliminary and exploratory nature of this randomized pilot trial, no formal power calculation was performed prior to enrollment. Instead, the sample size of 20 (10 participants per group) was determined based on feasibility and aligned with established recommendations for pilot studies. Such designs primarily aim to refine study procedures and generate effect size estimates to guide the planning of future large-scale, confirmatory clinical trials.

A CONSORT flow diagram (**Figure 7.**) summarizes the participant pathway throughout the study, including enrollment, randomization, group allocation, and inclusion in the final analysis.

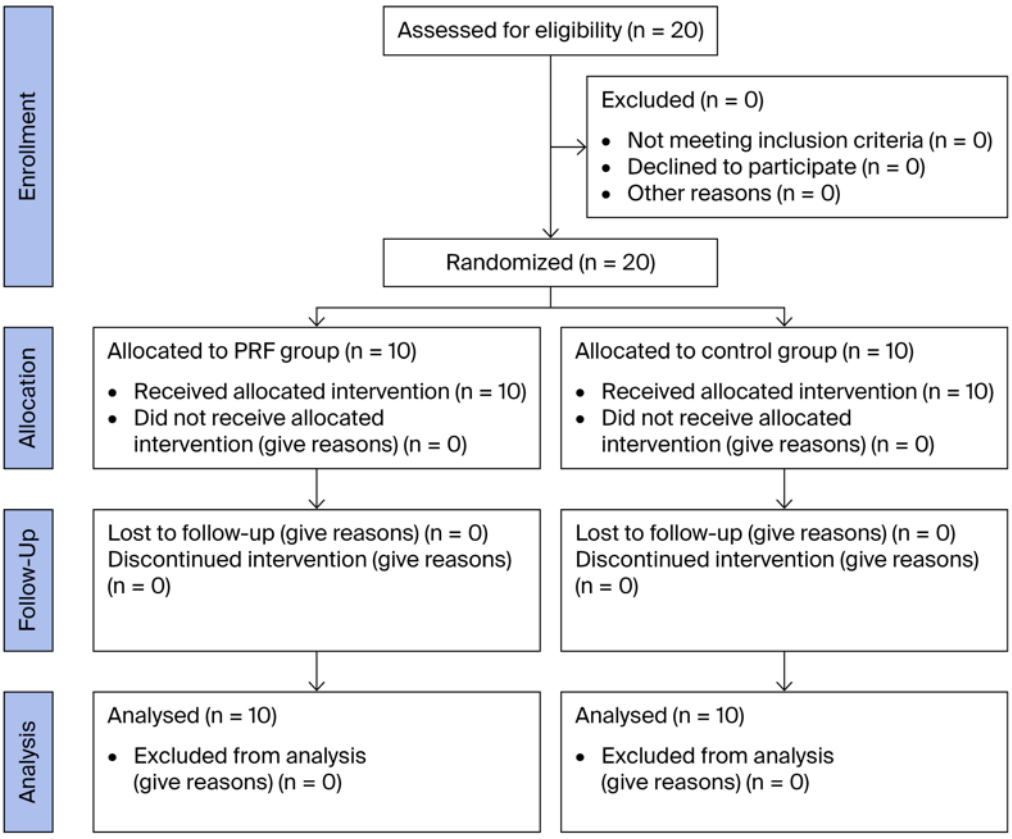

Figure 7. CONSORT flow diagram.

3.3. Case Report: Composite Use of A-PRF and Albumin-Coated Allograft in a Patient with Gorlin–Goltz Syndrome

3.3.1. Detailed Case Description

A 37-year-old male patient presented to the Department of Oro-Maxillofacial Surgery and Stomatology, Faculty of Dentistry, Semmelweis University, with a confirmed diagnosis of Gorlin–Goltz syndrome (nevoid basal cell carcinoma syndrome). The present case report was conducted in accordance with the ethical standards outlined in the Declaration of Helsinki. Prior to the initiation of any diagnostic or therapeutic procedures, the patient received comprehensive written and verbal information detailing the nature, objectives, potential risks, and benefits

of the proposed treatment. Informed consent was obtained, with clear communication that participation in the study was entirely voluntary and could be withdrawn at any stage without prejudice. This case description has been prepared in alignment with the CARE (Case Report) guidelines for the transparent and standardized reporting of clinical cases.[117]

In this patient, multiple cystic lesions were incidentally identified in both the mandible and maxilla during routine dental radiographic examination. Intraoral inspection revealed poor oral hygiene, generalized periodontitis, multiple missing teeth, and residual roots; however, no clinically visible signs of cystic involvement were observed in the oral cavity. Panoramic radiographs and cone-beam computed tomography (CBCT) imaging revealed the presence of four distinct cystic lesions affecting both jaws. The first and largest radiolucent lesion extended from the right mandibular condyle to the angle of the mandible. A second, bilocular osteolytic lesion was detected in the right mandibular body in the region of the molars. Additionally, two further cystic lesions were observed: one in the left mandibular body near the premolar region, and another in the maxilla, located between teeth 24 and 26, displacing the adjacent roots. Preoperative preparation included dental scaling, periodontal therapy, and comprehensive oral rehabilitation.

Due to the extensive nature of the cystic lesion involving the right mandibular ramus, decompression was selected as the initial therapeutic approach. Access was gained by creating bone windows through elevation of the mucoperiosteum and removal of bone in the retromolar region and along the alveolar crest. A specimen from the cystic lining was obtained for histopathological analysis, which confirmed the diagnosis of a parakeratinized odontogenic keratocyst (OKC). Following evacuation of the cystic contents, the cavity was packed with gauze soaked in 2% povidone–iodine for a period of three days. To maintain decompression, a custom drainage device was fabricated by a dental technician. This consisted of a silicone tube extending deep into the lesion, connected to an acrylic plate stabilized by the mandibular teeth. The patient was instructed to remove, clean, and replace the

device twice daily to ensure patency of the drainage. Over a period of 10 months, radiographic imaging demonstrated progressive reduction in lesion size. Based on these findings and the initial pathology report, complete enucleation of the cyst was performed, including removal of surrounding bone margins. Histological analysis of the resected specimen confirmed the initial diagnosis of OKC, characterized by a fibrous connective tissue wall lined with parakeratinized stratified squamous epithelium.

Primary enucleation was performed on all three remaining cysts, which were smaller in size and anatomically well positioned. The surgeries were carried out under local anesthesia (Ultracain DS Forte, Sanofi-Aventis, Paris, France). In the mandible, lingual paracrestal and buccal double-releasing incisions were made, while in the maxilla, palatal paracrestal and buccal releasing incisions were used. After flap elevation, complete enucleation was achieved with clear margins. The resulting osseous defects were grafted with a composite material comprising serum albumin-coated bone allograft (BoneAlbumin) and advanced platelet-rich fibrin (A-PRF). For A-PRF preparation, 40 mL of venous blood was drawn into four A-PRF+ tubes (Process for PRF, Nice, France) and centrifuged for 14 minutes at 1300 rpm using a Duo Quattro Centrifuge. The fibrin clots were then compressed in a PRF Box to obtain membranes. Fragments of the A-PRF membranes and the expressed plasma were mixed with 1.5–2 cm^3 of BoneAlbumin (Orthosera Dental Zrt, Győr, Hungary), and the resulting graft was packed into the bone cavities. The lateral bone window was covered with an A-PRF membrane, and flaps were closed using single interrupted non-resorbable sutures. Postoperative care included amoxicillin–clavulanic acid (1 g twice daily for 7 days), diclofenac (50 mg three times daily for 3 days), and 0.12% chlorhexidine mouthwash (twice daily for 7 days). Sutures were removed on the seventh postoperative day. No provisional prostheses were used during healing. CBCT scans were obtained at 3 and 6 months postoperatively for each surgical site. Implantation and biopsy were performed at 6 months in the left mandible and after 3 months in the right mandible and maxilla.

Following the appropriate healing periods, a total of eight dental implants were placed using a standardized protocol under local anesthesia (Ultracain DS Forte, Sanofi-Aventis, Paris, France). A mid-crestal incision was made, and a full-thickness mucoperiosteal flap was elevated to expose the surgical site. Bone-core biopsy samples were harvested using a custom-designed modular trephine drill (Full-Tech Kft, Szigetszentmiklós, Hungary) with an internal diameter of 2.5 mm, an external diameter of 3.25 mm, and a length of 10 mm. After sampling, implant site preparation was continued using the manufacturer's standard drilling sequence, and the implants (SGS P5D with SBCT surface, SGS Dental, Budapest, Hungary) were placed immediately thereafter. A two-stage healing protocol was followed, and flaps were closed using non-resorbable sutures. Postoperative care included a seven-day course of amoxicillin–clavulanic acid (1 g twice daily), diclofenac (50 mg three times daily for three days), and chlorhexidine mouthwash (twice daily for seven days). Sutures were removed on the seventh postoperative day. After a three-month osseointegration period, implant stability was assessed using resonance frequency analysis (RFA) with SmartPegs and the Osstell IDx device (Osstell AB, Göteborg, Sweden). Final prosthetic restorations were subsequently placed. Of the eight implants, four were inserted into previously augmented sites and four into native bone.

Following biopsy collection, the harvested bone-core samples were subjected to high-resolution microcomputed tomography (μCT) scanning using a Bruker 1272 X-ray microtomograph (Bruker μCT, Kontich, Belgium) (**Figure 8**).

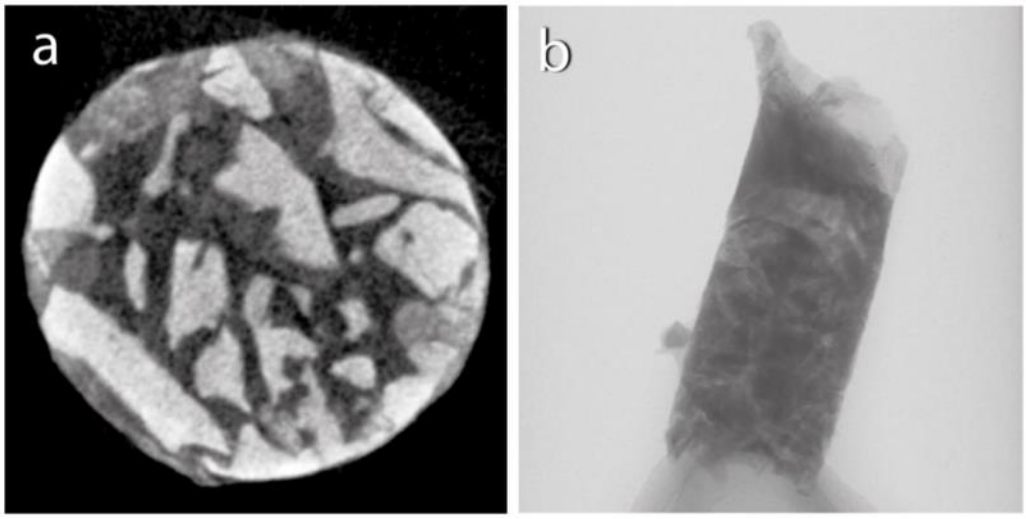

Figure 8. Micro-CT scan: (**a**) horizontal section; (**b**) vertical section.

Subsequent to µCT imaging, the samples underwent histological processing, and a histomorphometric analysis was performed by an independent, blinded examiner (**Figure 9**).

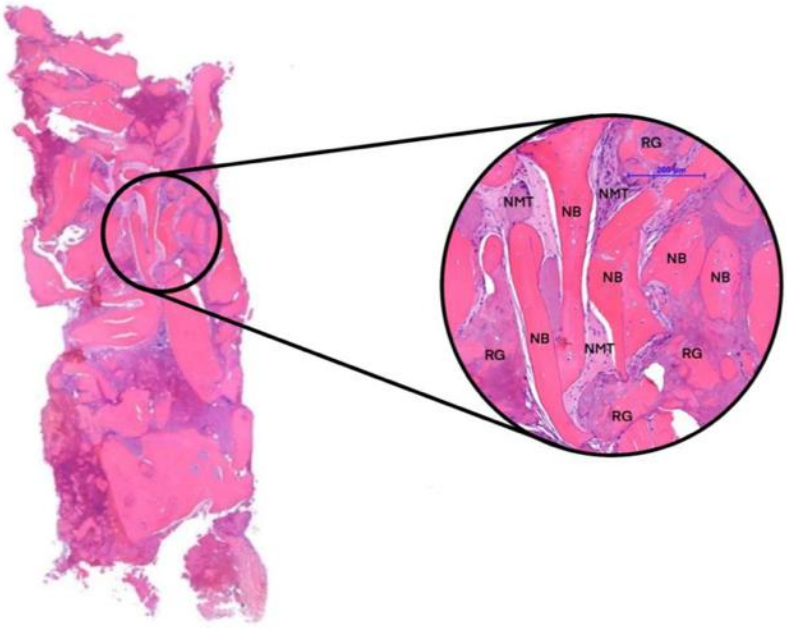

Figure 9. Histological section. Newly formed bone (NFB), residual graft particles (RGs), and non-mineralized tissue (NMT).

Both the three-month and six-month post-operative samples were evaluated. The analysis focused on the micromorphological characteristics of the specimens, specifically quantifying the proportions of newly formed bone (NFB) and residual graft particles (RGs). Definitions and descriptions of the relevant histomorphometric parameters utilized in the evaluation are detailed in **Table 1.**

Table 1. Definitions of the relevant morphometric variables.

Abbreviation	Variable	Description	Standard Unit
BV/TV	Bone volume fraction	Ratio of the segmented bone volume to the total volume of the region of interest	%
BS/TV	Bone surface density	Ratio of the segmented bone surface to the total volume of the region of interest	mm^{-1}
BS/BV	Specific bone surface	Ratio of the segmented bone surface to the segmented bone volume	mm^{-1}
Tb.Th	Trabecular thickness	Mean thickness of trabeculae assessed using direct 3D methods	mm
Tb.Sp	Trabecular separation	Mean distance between trabeculae assessed using direct 3D methods	mm
Tb.Pf	Trabecular bone-pattern factor	Index of connectivity of trabecular bone that calculates an index of the relative convexity or concavity of the total bone surface on the principle that concavity indicates connectivity (and the presence of 'nodes') and convexity indicates isolated disconnected structures (struts)	1/mm

Abbreviation	Variable	Description	Standard Unit
DA	Degree of anisotropy	DA is 1 ¼ isotropic and >1 ¼ anisotropic by definition; DA is ¼ the length of the longest divided by the shortest mean intercept length vector	None
SMI	Structure model index	An indicator of the structure of trabeculae; SMI is 0 for parallel plates and 3 for cylindrical rods	None
Po(op)	Open porosity	Percent open porosity is the volume of open pores as a percent of the total VOI volume	%
Po(tot)	Total porosity	Total porosity is the volume of all open plus closed pores as a percent of the total volume of the region of interest	%
Conn	Connectivity	An effective and efficient method to compute the Euler connectivity in three dimensions is the Conneulor. This algorithm gauges a property termed 'redundant connectivity', which is the extent to which different parts of the object are interconnected. It quantifies the maximum number of connections in a structure that can be cut before the entire structure splits into two disjointed segments	None

4. Results

The following section presents the outcomes of the three main investigations included in this dissertation. Each subchapter corresponds to one of the research components described in the Methods section: the validation of a 3D facial scanner for soft tissue analysis, a randomized controlled clinical trial evaluating the effects of PRF membranes on postoperative recovery after apicoectomy, and a case report involving the composite use of A-PRF and an albumin-coated bone allograft in a syndromic patient. Results are reported according to the predefined outcome measures and statistical methods, with a focus on both clinical and quantitative findings.

4.1. Validation of a 3D Facial Scanner for Craniofacial Anthropometry

Statistical analysis was performed using IBM SPSS Statistics for Windows, Version 25.0 (IBM Corp., Armonk, NY, USA). The normality of the data distribution was assessed using the Kolmogorov–Smirnov test. A 95% confidence interval and a significance level of $p < 0.05$ were defined a priori. For the comparison of paired measurements obtained from the same subjects, paired-samples t-tests were applied where the assumption of normality was met, while Spearman's rank correlation coefficient was used to evaluate associations between continuous variables.

The data did not significantly deviate from a normal distribution, supporting the use of parametric testing. This justified the use of paired-samples t-tests for the comparison of paired measurements.

The data from 11 subjects were analyzed. **Table 2** shows the mean caliper measurements of two examiners and the difference between them.

Table 2. The caliper measurements of two examiners and the difference between them.

	Examiner 1 (Caliper)	**Examiner 2 (Caliper)**	**Difference of the Means**	***t*-Test**	**Intraclass Correlation Coefficient (ICC)**
Glabella—Subnasale	66.73	66.91	−0.18	0.751	0.954 ***
Subnasale—Menton	69.94	68.53	1.41	0.001	0.990 ***
Nasion—Pronasale	45.16	45.25	−0.09	0.842	0.949 ***
Subnasale—Pronasale	20.98	21.32	−0.34	0.475	0.880 **
Exocanthion—Exocanthion	95.66	96.18	−0.52	0.263	0.990 ***
Cheilion—Cheilion	53.38	53.28	0.1	0.796	0.967 ***
Exocanthion Right—Cheilion Right	71.31	71.04	0.27	0.603	0.963 ***
Exocanthion Left—Cheilion Left	71.08	71.09	−0.01	0.984	0.960 ***
Gonion Left—Pogonion	86.01	85.44	0.57	0.255	0.992 ***

	Examiner 1 (Caliper)	Examiner 2 (Caliper)	Difference of the Means	*t*-Test	Intraclass Correlation Coefficient (ICC)
Gonion Right—Pogonion	85.00	84.34	0.66	0.128	0.993 ***
Alare-Alare	34.69	34.21	0.48	0.317	0.933 ***

** $p < 0.001$ *** $p < 0.0001$. Reliability: ICC < 0.4 (poor); 0.4 ≤ ICC < 0.75 (medium to good); ICC ≥ 0.75 (excellent).

The comparison of caliper measurements between the two examiners revealed no statistically significant differences, suggesting consistent measurement accuracy. A single exception was observed at the subnasale–menton distance, where a lower value was recorded by the second examiner.

The correlation analysis demonstrated statistically significant associations between the caliper-based measurements obtained by Examiner 1 and Examiner 2 across all reference distances, supporting the reliability and accuracy of the measurements. The resulting correlation coefficients indicated excellent consistency for the majority of variables. A moderate correlation was observed only in the case of the subnasale–pronasale measurement, suggesting slightly lower inter-examiner agreement for this specific parameter, though still within an acceptable range. The corresponding scanner-based measurement means and inter-examiner differences are presented in **Table 3.**

Table 3. Mean scanner measurements.

	Examiner 1 (Scanner)	Examiner 2 (Scanner)	Difference of the Means	*t*-Test	Intraclass Correlation Coefficient (ICC)
Glabella—Subnasale	67.41	67.54	−0.13	0.798	0.933 ***
Subnasale—Menton	70.45	70.05	0.4	0.192	0.992 ***
Nasion—Pronasale	44.82	44.65	0.17	0.713	0.948 ***
Subnasale—Pronasale	21.80	21.94	−0.14	0.674	0.922 ***
Exocanthion—Exocanthion	95.06	95.01	0.05	0.048	0.988 ***
Cheilion—Cheilion	53.06	53.13	−0.07	0.948	0.791 ***
Exocanthion Right—Cheilion Right	72.23	72.26	−0.03	0.924	0.986 ***
Exocanthion Left—Cheilion Left	71.26	70.69	0.57	0.177	0.974 ***
Gonion Left—Pogonion	86.98	86.31	0.67	0.080	0.994 ***

	Examiner 1 (Scanner)	Examiner 2 (Scanner)	Difference of the Means	*t*-Test	Intraclass Correlation Coefficient (ICC)
Gonion Right—Pogonion	84.93	84.71	0.22	0.522	0.995 ***
Alare-Alare	34.51	34.68	−0.17	0.682	0.946 ***

$p < 0.001$ *** $p < 0.0001$. Reliability: ICC < 0.4 (poor); 0.4 ≤ ICC < 0.75 (medium to good); ICC ≥ 0.75 (excellent).

The results indicated no statistically significant differences between the measurements obtained by the two examiners at any anatomical landmark. ICC analysis demonstrated high measurement reliability for all measured parameters, supporting the consistency and reproducibility of the measurements between observers.

Spearman's correlation analysis demonstrated strong associations between the measurements obtained by the two examiners. Together with the high ICC values, these findings support good inter-examiner reliability of the 3D scanner measurements.

Table 4 presents the comparison between the measurements obtained by Examiner 1 using the digital caliper and those obtained via 3D scanning, along with the differences between the two methods.

Table 4. Comparison of the results measured by Examiner 1.

	Examiner 1 (Caliper)	Examiner 1 (Scanner)	Difference of the Means	*t*-Test	Intraclass Correlation Coefficient (ICC)
Glabella—Subnasale	66.73	67.41	−0.68	0.050	0.978 ***
Subnasale—Menton	69.94	70.45	−0.51	0.193	0.989 ***
Nasion—Pronasale	45.16	44.82	0.34	0.360	0.970 ***
Subnasale—Pronasale	20.98	21.80	−0.82	0.124	0.860 **
Exocanthion—Exocanthion	95.66	95.06	0.6	0.346	0.982 ***
Cheilion—Cheilion	53.38	53.06	0.32	0.341	0.320 ***
Exocanthion Right—Cheilion Right	71.31	72.23	−0.92	0.048	0.970 ***
Exocanthion Left—Cheilion Left	71.08	72.23	−1.15	0.703	0.965 ***
Gonion Left—Pogonion	86.01	86.98	−0.97	0.063	0.990 ***

	Examiner 1 (Caliper)	Examiner 1 (Scanner)	Difference of the Means	*t*-Test	Intraclass Correlation Coefficient (ICC)
Gonion Right—Pogonion	85.00	84.93	0.07	0.834	0.998 ***
Alare-Alare	34.69	34.51	0.18	0.749	0.904 ***

** $p < 0.001$ *** $p < 0.0001$. Reliability: ICC < 0.4 (poor); 0.4 ≤ ICC < 0.75 (medium to good); ICC ≥ 0.75 (excellent).

No statistically significant differences were observed between the measurements obtained by Examiner 1 using the caliper and the 3D scanner, except for the right exocanthion–right cheilion distance (p = 0.048).

The ICC values generally indicated good reliability between caliper and scanner measurements. Lower reliability was observed for the subnasale–pronasale and cheilion–cheilion distances, suggesting reduced consistency between the two measurement methods for these specific parameters. **Table 5** shows the measurements done by Examiner 2 with caliper and scanner, and the difference between them.

Table 5. Comparison of the results measured by Examiner 2.

	Examiner 2 (Caliper)	Examiner 2 (Scanner)	Difference of the Means	*t*-Test	Intraclass Correlation Coefficient (ICC)
Glabella—Subnasale	66.91	67.54	−0.63	0.270	0.937 ***
Subnasale—Menton	68.53	70.05	−1.52	0.005	0.983 ***
Nasion—Pronasale	45.25	44.65	0.6	0.289	0.928 ***
Subnasale—Pronasale	21.32	21.94	−0.62	0.053	0.935 ***
Exocanthion—Exocanthion	96.18	95.01	1.17	0.685	0.991 ***
Cheilion—Cheilion	53.28	53.13	0.15	0.878	0.800 *
Exocanthion Right—Cheilion Right	71.04	72.26	−1.22	0.009	0.978 ***
Exocanthion Left—Cheilion Left	71.09	70.69	0.4	0.510	0.943 ***
Gonion Left—Pogonion	85.44	86.31	−0.87	0.116	0.989 ***

	Examiner 2 (Caliper)	Examiner 2 (Scanner)	Difference of the Means	*t*-Test	Intraclass Correlation Coefficient (ICC)
Gonion Right—Pogonion	84.34	84.71	−0.37	0.426	0.991 ***
Alare-Alare	34.21	34.68	−0.47	0.281	0.928 ***

$p < 0.05$ * $p < 0.001$ *** $p < 0.0001$. Reliability: ICC < 0.4 (poor); 0.4 ≤ ICC < 0.75 (medium to good); ICC ≥ 0.75 (excellent).

In the case of Examiner 2, statistically significant differences were identified between caliper and scanner measurements at two anatomical reference points—specifically the subnasale–menton and exocanthion right–cheilion right distances. These discrepancies may be attributed either to the examiner's limited experience or to the inherent complexity of these regions for manual measurement. Examiner 2's caliper values were generally lower than those recorded by the scanner. A similar trend was observed for Examiner 1, though the differences were less pronounced.

The correlation analysis demonstrated generally strong associations between caliper-based and scanner-based measurements. However, a weaker relationship was observed for the cheilion–cheilion measurement, indicating lower consistency between the two measurement methods for this specific parameter.

When comparing the two measurement modalities, a mean deviation of −0.36 mm ± 1.52 mm was observed (range: −3.79 to 4.90 mm), suggesting that the scanner produces clinically acceptable results within a narrow margin of error.

Table 6 summarizes the duration of the measurement procedures. For the direct caliper-based technique, the average measurement time was 2 minutes and 25 seconds for the experienced examiner, and 2 minutes and 53 seconds for the inexperienced examiner. In contrast, the 3D scanning workflow was segmented into three distinct phases: (1) scanning, (2) post-processing of the image data, and (3) conducting measurements on the resulting 3D mesh. Across all phases, the experienced examiner consistently completed the tasks more quickly than the inexperienced examiner. Notably, the actual scanning phase required less time than the direct caliper measurements for both examiners: 1 minute and 18 seconds for the experienced examiner and 1 minute and 40 seconds for the inexperienced examiner. This indicates that 3D scanning, even when factoring in additional processing time, has the potential to offer greater time efficiency, particularly with increased operator experience. **(Table 6.)**

Table 6. Comparison of the measurements times.

Examiner 1 (caliper)	02:25	Examiner 2 (caliper)	02:53
Examiner 1 (scanner) sum	08:04	Examiner 2 (scanner) sum	08:58
Scanning time	01:18	Scanning time	01:40
Image processing	05:14	Image processing	05:35
Measurement on mesh	01:30	Measurement on mesh	01:42

A comparison between direct caliper-based measurements and those obtained through 3D facial scanning reveals several important distinctions. While calipers represent a cost-effective method for acquiring linear facial dimensions, their

application is time-consuming and requires the physical presence of the patient. Additionally, the use of calipers may lead to soft-tissue compression, introducing potential inaccuracies in the measurements. In contrast, 3D scanning—despite its higher initial cost—enables a more efficient workflow by facilitating indirect measurements on virtual models, following a single acquisition and post-processing phase. This approach eliminates the need for patient presence during subsequent measurements and minimizes errors associated with tissue deformation. Further advantages of 3D scanning include the ability to store and export digital models, remeasure arbitrary anatomical points retrospectively, and accurately capture complex soft-tissue topography. The key advantages and limitations of both methods are summarized in **Table 7.**

Table 7. Comparison of the measurements.

	Measurement with Caliper	**3D Scanning**
Price of the device	Inexpensive	Higher-priced
Method of measurement	Direct	Indirect—on a virtual model
Time of the measurement	Time-consuming	1. Relatively fast scanning 2. Post-processing 3. Indirect measurement
Reproducibility	Presence of the patient required	Repeated measurements on a 3D model are possible
Possible causes of measurement error	Tissue distortion during measurement	Motion artifacts

	Measurement with Caliper	3D Scanning
Other benefits	-	• Data storage and exportation • Subsequent measurement of arbitrary points • Accurate mapping of soft tissue and areas with complex morphology

4.2. Randomized Controlled Clinical Trial: The Effect of PRF on Postoperative Outcomes after Apicoectomy

4.2.1. Baseline Characteristics

The baseline demographic and clinical parameters of the study population are presented in **Table 8** and **Table 9**. There were no statistically significant differences between the PRF and control groups regarding age, with mean values of 40.3 ± 7.51 years and 43.9 ± 7.43 years, respectively. While the sex distribution varied between the groups—six males and four females in the PRF group versus two males and eight females in the control group—this difference was not statistically evaluated as part of the pilot study.

Health-related quality of life, assessed using the PROMIS-29+2 Profile v2.1 at baseline, showed no significant differences across any domain. For instance, physical function scores were identical in both groups (18.7 ± 1.88 vs. 18.7 ± 2.58; $p = 1.000$), and anxiety levels were comparable (7.9 ± 3.98 vs. 8.4 ± 3.86; $p = 0.779$). These findings indicate that the two groups had similar baseline characteristics, supporting the internal validity of subsequent comparative analyses.

Table 8. Baseline (T0) quality-of-life dimensions.

Dimension	Points	Case Group (Mean ± Standard Deviation)	Control Group (Mean ± Standard Deviation)	95% CI		*p* Value
				Lower	Upper	
Physical function	20	18.7 ± 1.88	18.7 ± 2.58	−2.126	2.126	1.000
Anxiety	20	7.9 ± 3.98	8.4 ± 3.86	−4.187	3.187	0.779
Emotional stress	20	6.1 ± 2.80	6.7 ± 2.62	−3.153	1.953	0.628
Fatigue	20	9.0 ± 3.24	9.9 ± 4.06	−4.488	2.688	0.604
Sleep disturbance	20	9.9 ± 3.44	9.6 ± 1.64	−2.237	2.837	0.807
Social tasks	20	16.9 ± 4.20	17.4 ± 4.01	−4.356	3.356	0.788
Pain interference	20	8.4 ± 4.81	8.3 ± 5.18	−4.602	4,.802	0.965
Cognitive function	10	7.6 ± 1.89	7.3 ± 2.16	−1.611	2.211	0.745
Total score	150	83.5 ± 8.90	86.3 ± 8.23	−2.277	12.721	0.147

Abbreviations: CI—confidence interval; *p*—probability value.

Table 9. Baseline demographic characteristics of the PRF and control groups.

Variable	PRF Group (n = 10)	Control Group (n = 10)
Age (Years)	40.3 ± 7.51	43.9 ± 7.43
Sex (M/F)	6/4	2/8

Abbreviations: n—number of participants; M/F—male/female.

4.2.2. Postoperative Quality of Life

On postoperative day 7, patients in the PRF group demonstrated significantly better health-related quality of life outcomes across multiple PROMIS-29+2 domains when compared to the control group. As detailed in **Table 10**, the PRF group reported higher physical function, reduced pain interference, improved sleep quality, and enhanced participation in both social and cognitive activities.

These results indicate that the application of PRF membranes may contribute to improved early postoperative recovery and support a more favorable patient-reported outcome profile in the short term.

Table 10. Postoperative (T1, day 7 post-operation) quality-of-life dimensions.

Dimension	Points	Case Group (Mean ± Standard Deviation)	Control Group (Mean ± Standard Deviation)	95%CI		*p* Value
				Lower	Upper	
Physical function	20	19.4 ± 0.84	16.2 ± 4.26	0.3125	6.087	0.032
Anxiety	20	5.5 ± 1.71	7.9 ± 4.17	−5.399	0.599	0.110
Emotional stress	20	4.6 ± 0.84	7.1 ± 3.47	−4.877	−0.122	0.040
Fatigue	20	7.1 ± 2.46	9.6 ± 3.56	−5.381	0.381	0.085
Sleep disturbance	20	7.9 ± 2.37	10.9 ± 2.13	−5.121	−0.878	0.008
Social tasks	20	18.7 ± 1.9	14.9 ± 3.47	1.151	6.448	0.007
Pain interference	20	5.9 ± 2.02	10.2 ± 3.19	−6.810	−1.789	0.002
Cognitive function	10	9.5 ± 0.70	7.7 ± 1.70	0.574	3.025	0.006
Total score	150	78.6 ± 6.00	84.5 ± 6.65	−2.918	6.518	0.411

Abbreviations: CI—confidence interval; *p*—probability value.

4.2.3. Postoperative Pain Assessment

Postoperative pain was evaluated daily for seven consecutive days using the Visual Analog Scale (VAS). As illustrated in **Figure 10**, the PRF group exhibited significantly lower mean pain intensity scores (1.80 ± 1.22) compared to the control group (3.80 ± 2.44). This difference reached statistical significance ($p = 0.034$), with a 95% confidence interval ranging from −3.82 to −0.18, indicating that the effect was both statistically and clinically meaningful. The associated test statistics were $F = 5.233$, $t = -2.315$, and degrees of freedom (df) = 18.

These findings suggest that the use of PRF membranes may contribute to more effective postoperative pain management during the early recovery period.

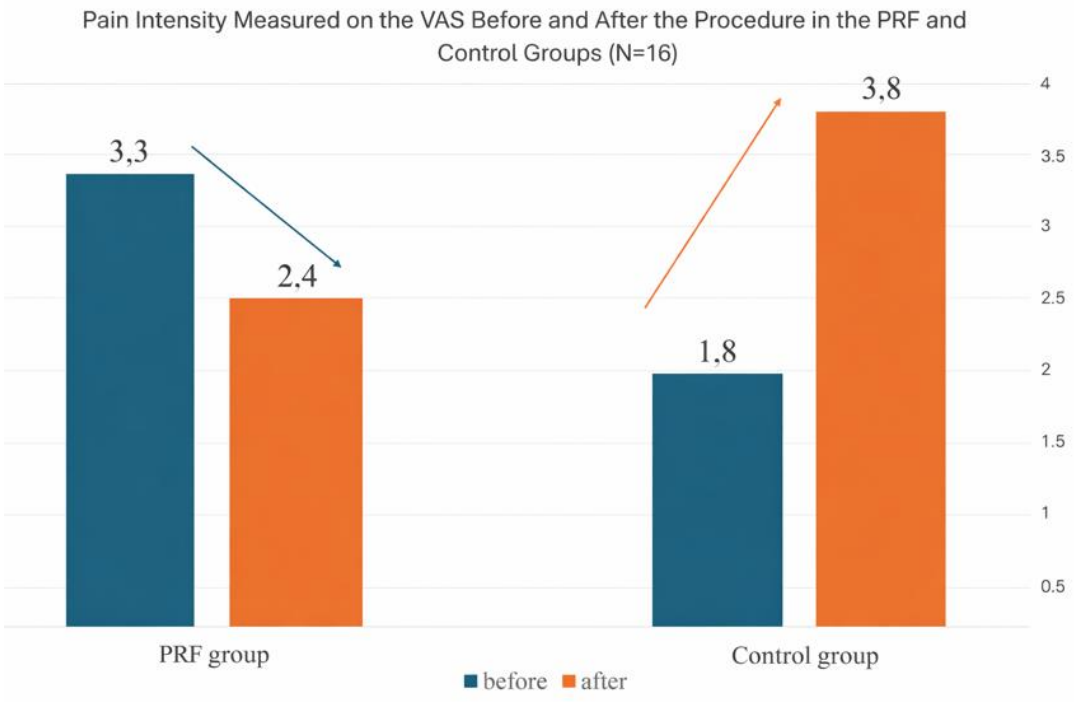

Figure 10. Comparison of postoperative VAS pain scores in the PRF and control groups. Error bars represent standard deviations. * indicates a statistically significant difference between groups in postoperative pain ($p = 0.034$, independent-samples t-test).

4.2.4. Postoperative Swelling

Facial swelling was quantitatively assessed on postoperative day 3 using three-dimensional surface scanning and volumetric analysis. As presented in **Table 11**, patients in the PRF group demonstrated significantly lower mean swelling volumes (15.93 ± 4.12 cm^3) compared to those in the control group (23.05 ± 8.22 cm^3). This difference was statistically significant ($p = 0.025$), indicating that the application of PRF membranes may help reduce soft-tissue inflammation and support improved healing during the early postoperative period.

Table 11. Volumetric analysis of swelling.

Group	Volume, cm^3 (Mean ± Standard Deviation)	Mean Volume Difference (cm^3)	95% CI		*p* Value
			Lower	Upper	
Case group	15.93 ± 4.12	7.12	−13.227	−1.013	0.025
Control group	23.05 ± 8.22				

Abbreviations: CI—confidence interval; *p*—probability value.

4.2.5. Correlation Analysis Results

A correlation analysis was conducted to evaluate the association between postoperative facial swelling and patient-reported outcomes from the PROMIS-29+2 quality-of-life domains. As presented in **Table 12**, a statistically significant negative correlation was identified between swelling volume and sleep disturbance scores within the PRF group ($r = -0.705$; $p < 0.05$). This finding indicates that increased facial swelling was associated with reduced sleep quality. No other

statistically significant correlations were observed between swelling and the remaining PROMIS domains in either the PRF or control groups.

Table 12. Correlation between swelling and quality-of-life dimensions.

Dimension	Correlation Coefficient (r)	*p* Value
Sleep disturbance	−0.705	<0.05
Others	Nonsignificant	

Abbreviations: r—correlation coefficient; *p*—probability value.

4.2.6. Adverse Events

No adverse events were reported in either the PRF or control groups throughout the study period. All patients completed the postoperative follow-up without complications, and no unexpected medical or surgical issues occurred. Adverse events were prospectively monitored and included postoperative infection, secondary bleeding, wound dehiscence, allergic reactions, delayed healing, and systemic complications such as fever or hospitalization. None of these events were observed in any participant, indicating that both treatment protocols were well tolerated.

4.3. Case Report: Composite Use of A-PRF and Albumin-Coated Allograft in a Patient with Gorlin–Goltz Syndrome

Bone-core biopsy samples were collected from each implant site and analyzed using microcomputed tomography (μCT), followed by micromorphometric and histological evaluation. The analyzed specimens included samples from augmented areas after 3 and 6 months of healing, as well as native bone for reference. The micromorphometric parameters derived from the μCT scans are presented in **Table 13**.

Table 13. Results of the micromorphometric analysis.

Abbreviation	Sample	*n*	Mean
BV/TV	3 months of healing	2	25.7886
	6 months of healing	2	39.7210
	Native bone	4	41.0630
BS/BV	3 months of healing	2	0.0317
	6 months of healing	2	0.018.6
	Native bone	4	0.0146
BS/TV	3 months of healing	2	0.0069
	6 months of healing	2	0.0067
	Native bone	4	0.0059
Tb.Th	3 months of healing	2	151.8090
	6 months of healing	2	210.2448
	Native bone	4	216.2362
Tb.Sp	3 months of	2	316.6615

Abbreviation	Sample	*n*	Mean
	healing		
	6 months of healing	2	300.3770
	Native bone	4	256.2631
Tb.Pf	3 months of healing	2	0.0080
	6 months of healing	2	0.0055
	Native bone	4	0.0017
DA	3 months of healing	2	1.1206
	6 months of healing	2	1.1882
	Native bone	4	1.5026
SMI	3 months of healing	2	1.4071
	6 months of healing	2	1.9613
	Native bone	4	0.7452
Po(tot)	3 months of healing	2	74.2112
	6 months of	2	60.2789

Abbreviation	Sample	*n*	Mean
	healing		
	Native bone	4	58.9067
Po(op)	3 months of healing	2	74.2022
	6 months of healing	2	60.2427
	Native bone	4	58.9067
Conn	3 months of healing	2	1641.5
	6 months of healing	2	2160.5
	Native bone	4	1131.4

Subsequent to µCT imaging, the biopsies underwent routine histological processing. Histological examination confirmed gradual resorption and remodeling of the graft material in the augmented regions, without evidence of inflammation or foreign-body reaction. Manual segmentation was used to quantify the proportions of newly formed bone (NFB), residual graft particles (RGs), and non-mineralized tissue (NMT). Native bone (NB) was excluded from the analysis of augmented samples. The results of the histomorphometric analysis are summarized in **Table 14**.

Table 14. Results of the histomorphometric analysis. The percentages of newly formed bone (NFB), residual graft particles (RGs), and non-mineralized tissue (NMT) were determined based on manual segmentation.

Groups	*n*	NFB	NMT	RG
3 months of healing	2	40.59%	30.82%	28.59%
6 months of healing	2	55.92%	27.95%	16.13%
Native bone (NB)	4	60.78%	39.22%	-

5. Discussion

5.1. Overview and Principal Findings

This dissertation aimed to explore the clinical applicability and biological effects of platelet-rich fibrin (PRF) in oral and maxillofacial surgery,[54,57] while also validating a novel 3D facial scanning system for objective soft tissue assessment.[82] The research was structured into three complementary components: a 3D scanner validation study, a randomized controlled clinical trial evaluating PRF's influence on postoperative recovery after apicoectomy, and a case report on composite bone augmentation using A-PRF and albumin-coated allograft in a syndromic patient.

The 3D scanner validation study demonstrated that non-invasive digital facial scanning provides reproducible and clinically acceptable measurements when compared to traditional caliper-based anthropometry. The scanner proved to be a reliable tool for quantifying facial dimensions, with the added benefit of allowing post-procedural analysis, although the overall digital workflow required more time than direct anthropometric measurement.[82]

The randomized clinical trial showed that the application of PRF membranes during apicoectomy was associated with significantly better postoperative outcomes. Patients in the PRF group experienced reduced facial swelling, lower pain intensity, and improved quality of life in the first postoperative week. These findings suggest a potential beneficial effect of PRF on early postoperative recovery and patient comfort.[54]

In the case report involving a patient with Gorlin–Goltz syndrome, composite grafting using A-PRF and BoneAlbumin demonstrated favorable outcomes in terms of bone regeneration. Histomorphometric and μCT analyses demonstrated new bone

formation and the presence of residual graft particles without signs of inflammation, providing descriptive evidence of bone remodeling in the augmented areas.[57]

Together, the findings across all three components provide further evidence regarding the potential clinical applications of PRF and 3D imaging technologies in oral surgery and postoperative assessment.

5.2. Interpretation of Findings in the Context of the Literature

5.2.1. Clinical Interpretation of 3D Scanner Validation Results

The first part of this dissertation involved the validation of a portable, structured light-based 3D facial scanner (EINSTAR, Shining 3D, Hangzhou, China) for use in craniofacial anthropometry. In the field of maxillofacial surgery, the use of three-dimensional (3D) surface scanning has become increasingly prevalent in various clinical phases, including diagnosis, surgical planning, and postoperative follow-up [118-120]. Among the most frequently studied and validated photogrammetric systems are the 3dMD and Vectra platforms, which are widely regarded as gold standards for facial imaging [121-123]. Maal et al. evaluated different registration protocols for 3D facial photography in the context of oral and maxillofacial surgery. Their findings showed that surface-based registration, particularly when applied to pre-processed images, offered high levels of accuracy.[123] Moreover, both the Maxilim software and 3dMD software v3.0 demonstrated comparable precision, although a slight decrease in accuracy was noted with changes in facial expression. Similarly, Camison et al.[86] performed a validation study comparing the handheld Vectra H1 system to the 3dMDfacesystem. The results indicated that the Vectra H1 produced highly comparable measurements, with an average technical error of 0.84 mm and a root mean square (RMS) error of 0.43 mm. These data support the conclusion that the Vectra H1 system provides sufficient accuracy for most clinical applications in facial anthropometry and maxillofacial analysis. [82]

Craniofacial anthropometry remains a fundamental tool in both dentistry and maxillofacial surgery, offering valuable insights into facial morphology and growth dynamics. Zhang et al. employed 3D white-light scanning to evaluate nasolabial unit development in a cohort of 528 Chinese children. Their findings revealed that the most rapid growth occurred between birth and two years of age, with comparable patterns observed across sexes.[124,125] Facial morphology also plays a crucial role in the early recognition of genetic syndromes. Hammond et al. emphasized the utility of computer-based three-dimensional facial models in dysmorphology education, clinical diagnostics, and integrative genotype–phenotype research.[126] Furthermore, three-dimensional imaging has been validated as a reliable tool in the planning and outcome assessment of orthodontic and orthognathic surgical procedures. Hayeer et al. evaluated a novel volumetric facial assessment technique using stereophotogrammetric models and a digital analysis software. They identified the “tetrahedron formation” method as the most accurate, reporting minimal measurement error when image acquisition was performed under standardized facial expression conditions.[127]

The aim of the present study was to validate the EINSTAR 3D scanner (Shining 3D, Hangzhou, China) for clinical use in craniofacial applications. Specifically, the scanner was evaluated for its suitability in facial imaging related to maxillofacial surgical research, including preoperative planning and postoperative outcome assessment in orthognathic and cleft lip surgery. Additionally, its application in the objective evaluation of postoperative swelling was also explored, supporting its broader integration into clinical practice.[82]

To validate the scanner's accuracy, conventional direct anthropometric measurements using a digital caliper were compared with indirect measurements performed on 3D facial scans. Distances were recorded between predefined soft tissue landmarks. Previous research has demonstrated that the use of clearly defined facial landmarks enhances the precision of anthropometric assessments. In a validation study by Franco de Sa Gomes et al., craniofacial measurements

performed with an Artec Eva 3D light scanner on 15 subjects showed improved accuracy when reference points were physically marked, yielding approximately 1 mm accuracy with marks and around 2 mm without them. The study also reported excellent reliability, with intraclass correlation coefficients (ICC) ranging from 0.92 to 0.97, although scanning and processing required approximately twice the time of conventional caliper-based methods.[94,98]

When comparing direct caliper-based measurements with those obtained via 3D scanning, the analysis revealed a mean deviation of −0.36 mm ± 1.52 mm, with a range spanning from −3.79 to 4.9 mm. This level of deviation is within an acceptable clinical range and reflects the scanner's reliability for facial anthropometry. Similarly, in a study by Weinberg et al., 3D anthropometric measurements were performed on static mannequin heads, and the observed discrepancies between repeated measurements were consistently below 1 mm, further supporting the precision of three-dimensional surface imaging for standardized assessments.[128]

In a validation study assessing the clinical applicability of 3D surface scanners, comparative measurements were conducted using two different devices (Artec and Sense) against the Vectra system as a reference standard. The findings indicated that the Artec scanner demonstrated a mean deviation of 0.13 ± 2.71 mm (range: −10.26 to 13.93 mm), while the Sense scanner showed a mean deviation of −0.19 ± 3.81 mm (range: −14.09 to 18.92 mm) when compared to the reference measurements. These results highlight the variability between different 3D scanning technologies and underscore the importance of device-specific validation for clinical implementation.[107]

The comparative analysis of results obtained by two examiners—one experienced and one inexperienced—using both caliper-based and 3D scanning methods revealed generally consistent measurements across both techniques. However, a statistically significant discrepancy was identified in the subnasale–menton distance

when measured with the caliper. This variation is likely attributable to differences in the amount of pressure applied to mobile soft tissue landmarks, a known limitation of direct anthropometry. Aside from this isolated inconsistency, the measurements obtained by the two examiners were generally consistent, supporting the reliability of the 3D scanning approach across different user experience levels.[94]

Upon comparison of the measurements obtained by each examiner using both direct and indirect methods, it was observed that distances recorded via caliper (direct anthropometry) were generally shorter than those captured through 3D scanning. This trend aligns with previous findings reported in the literature. Notably, statistically significant discrepancies were detected in only two cases for the inexperienced examiner specifically in the right exocanthion–right cheilion and subnasale–menton distances. The intrarclass correlation coefficients (ICCs) for the cheilion–cheilion distance revealed a weak correlation for the experienced examiner (ICC: 0.32), while the inexperienced examiner demonstrated a more favorable, though still moderate, correlation (ICC: 0.8). These variations may, in part, be attributed to the inherent challenges of conducting measurements on live human subjects, where factors such as involuntary facial movements, variability in facial expressions, and the complexity of soft-tissue contours can introduce greater measurement error. Such inconsistencies are particularly prominent in the perioral region, which is known to exhibit high morphological variability and sensitivity to soft-tissue distortion.[89,94,101,129]

Consistent with previous findings reported by Koban et al. [27], the overall duration of the scanning procedure including acquisition, post-processing, and digital measurement was longer than that of direct anthropometric measurement. However, when isolating the scanning time itself, the process proved to be more time-efficient than caliper-based measurement, even for investigators without prior experience. This highlights the procedural efficiency of 3D scanning when considering the actual image acquisition phase, despite the additional time required for digital post-processing.[107]

Although the overall duration of 3D scanning is longer compared to traditional methods, this surface-based technique offers distinct advantages in the context of facial and maxillofacial surgery. It enables highly accurate digital modeling of the patient's facial soft tissues, including anatomically complex regions such as the ears, nose, and lips. This level of precision makes 3D scanning particularly well-suited for clinical applications requiring detailed surface mapping. Furthermore, it facilitates three-dimensional measurements with virtually unlimited flexibility, allowing clinicians to perform repeated assessments, store and export digital data, and build longitudinal databases for future research and treatment planning.[118]

Despite the notable advantages of facial scanning technology, several limitations and practical challenges must be acknowledged. A primary concern is the high initial investment required for the acquisition of scanning equipment, which may limit accessibility in certain clinical settings. Additionally, although the accuracy of facial scanning is generally reliable, various factors such as patient movement, motion artifacts, or discomfort during the scanning process can compromise the quality of the captured data. Addressing these limitations may require further technological refinements and continued research in the field of medical imaging. [130]

5.2.2. Effect of PRF on Postoperative Outcomes after Apicoectomy

The findings of this preliminary randomized controlled trial suggest that the application of platelet-rich fibrin (PRF) membranes may improve postoperative recovery following apicoectomy. Compared to conventional surgical treatment, patients who received PRF demonstrated a tendency toward reduced facial swelling, lower postoperative pain levels, and better health-related quality of life in the early healing period. These results support the hypothesis that PRF could contribute to enhanced healing and patient recovery after periapical surgery, warranting further investigation in larger-scale studies.[54]

Several prior studies have described the potential clinical benefits of platelet-rich fibrin (PRF) in enhancing soft-tissue healing and reducing postoperative discomfort. Fan et al. [8], for example, provided a detailed overview of PRF applications in oral and maxillofacial procedures, emphasizing its ability to modulate inflammation and promote tissue regeneration. In a systematic review and meta-analysis, Sinha et al. [48] reported that PRF may reduce postoperative pain and support healing in periapical surgery, primarily through the gradual release of growth factors. The biological mechanisms proposed in these studies are consistent with those described by Dohan et al. [2], who emphasized PRF's capacity to deliver bioactive molecules that facilitate soft-tissue repair. Additionally, a randomized clinical trial by Meschi et al. [131] found that combining PRF with an occlusive membrane was associated with improved outcomes in both bone regeneration and soft-tissue healing in root-end surgery.

Recent developments in platelet-rich fibrin (PRF) technology have led to the introduction of antibiotic-loaded PRF (AL-PRF), a formulation that incorporates antimicrobial agents into the fibrin matrix to enable localized drug delivery while maintaining the autologous and bioactive properties of PRF. A recent systematic review of in vitro studies reported that AL-PRF may inhibit bacterial growth and potentially improve the mechanical stability of the fibrin scaffold [29]. However, the preparation methods remain non-standardized, and clinical data are currently limited. While AL-PRF was not utilized in the present study and none of the participants required systemic antibiotic therapy this emerging approach may hold promise for future applications in endodontic microsurgery. Further clinical investigations are warranted to determine whether AL-PRF can offer additional benefits beyond those observed with conventional PRF membranes.[44,54]

With regard to patient-reported outcomes, the present findings are in accordance with those reported by Mubarak et al. [66], who highlighted the beneficial effects of PRF on patient comfort and postoperative quality of life. In the current study, these subjective improvements were assessed using the PROMIS-29+2 Profile, a

validated multidimensional instrument capable of capturing both physical and psychosocial aspects of recovery. The application of this tool extends the existing literature by providing a structured and comprehensive approach to patient-centered outcome evaluation. Previous studies have confirmed the reliability and relevance of PROMIS instruments in oral surgery settings, thereby supporting their integration into the present trial's assessment framework.[114,132]

In addition, the use of 3D optical imaging for the assessment of postoperative facial swelling, as employed in the present study, is supported by previous validation studies. Buitenhuis et al. and others have demonstrated that volumetric facial scanning yields reliable and reproducible measurements, particularly in the context of postoperative evaluation. [82,116] These findings reinforce the methodological robustness of our approach and support the use of 3D surface scanning as an objective tool for monitoring soft-tissue changes during the recovery period.

The findings of this pilot study suggest that PRF membranes could serve as a beneficial adjunct in periapical surgical procedures by supporting early postoperative recovery. The reduction in facial swelling, lower reported pain levels, and improvements in patient-reported quality-of-life indicators observed in the PRF group underscore the potential clinical relevance of this approach. These results are in agreement with previous studies that have highlighted the capacity of PRF to promote soft-tissue regeneration, modulate inflammatory responses, and alleviate postoperative discomfort. Additionally, PRF has demonstrated consistent regenerative potential in the treatment of intrabony periodontal defects, as documented in systematic reviews. In this context, Liu et al.presented a detailed classification of PRF-derived biomaterials and emphasized their applicability as bone graft substitutes in maxillofacial regenerative therapies.[8,18,48,54,133]

From a clinical perspective, PRF represents an autologous, cost-effective biomaterial that can be prepared chairside using simple protocols and without the need for chemical additives [8,18]. Its biological compatibility and ease of

application make it a practical option for routine use in surgical endodontic procedures. Previous studies have demonstrated favorable outcomes with PRF in oral surgery. For example, Al-Hamed et al. [55] and Ramos et al. [133] reported enhanced healing and reduced postoperative morbidity in third-molar extractions following PRF application—findings that are consistent with the present results observed in a periapical surgical setting. In addition, evidence from Praganta et al. [56] supports the clinical benefits of advanced PRF formulations in reducing postoperative swelling and pain in various oral surgical procedures.

Furthermore, the use of validated patient-reported outcome measures such as the PROMIS-29+2 Profile aligns with contemporary standards in patient-centered clinical research. The observed improvements in sleep quality, physical function, and social participation in the PRF group are consistent with earlier studies highlighting the potential of PRF to positively influence postoperative quality of life. [66,134]

Taken together, these findings support further investigation of PRF membranes as a potential adjunct in periapical surgery, particularly with regard to early postoperative morbidity and patient-reported outcomes.

Although this study was conducted within a single academic center using a standardized protocol, the results may hold broader clinical relevance. PRF membranes are autologous, relatively low-cost materials that can be prepared chairside using minimal equipment, which may facilitate their clinical application across different healthcare settings. [8] Further clinical research is warranted to explore their applicability across a wider range of oral surgical interventions and in diverse healthcare contexts, in order to determine the consistency of outcomes across different patient populations and clinical settings.

5.2.3. Composite Use of A-PRF and BoneAlbumin in Bone Regeneration

This case report aimed to explore treatment options for a patient diagnosed with multiple odontogenic keratocysts (OKCs) associated with Gorlin–Goltz syndrome and to evaluate the regenerative capacity of a composite graft composed of BoneAlbumin and advanced platelet-rich fibrin (A-PRF) following cyst enucleation. To assess the healing dynamics, both micromorphometric and histomorphometric analyses were performed on biopsy samples taken from the augmented regions.[57]

The findings provide preliminary observations on bone regeneration following the combined use of BoneAlbumin and A-PRF in the form of sticky bone after cystectomy. Notably, the tissue characteristics observed after a 3-month healing period were comparable to those typically seen after 6 months of healing using conventional protocols. These observations provide preliminary evidence that warrants further investigation of whether this composite graft may permit earlier implant placement. However, as these results are based on a single case, further studies are required to confirm the consistency and reliability of the observed regenerative outcomes.[57]

Complete surgical removal remains the primary strategy for managing odontogenic keratocysts to minimize the risk of recurrence. Following cystectomy, the resultant bony defects may be left to heal spontaneously or filled with autologous bone or bone substitute materials to support regeneration.[135] Bone defects in the maxillofacial region present unique regenerative dynamics due to the interplay of continuous bone resorption and apposition. The healing potential is influenced by multiple factors, including defect size, anatomical site, patient age, and systemic conditions. Among these, the size of the defect plays a critical role in determining the extent of natural consolidation. The concept of a critical size defect (CSD), originally defined by Schmitz et al., refers to a defect that does not heal completely without grafting, regardless of the observation period.[136] In line with this, it has been proposed that cystic lesions exceeding the dimensions of a CSD are unlikely to

undergo complete spontaneous regeneration. Supporting this, Schlegel et al. found that monocortical defects measuring 10 × 10 mm remained incompletely healed even after 52 weeks in an animal model when left ungrafted.[137]

In bone regeneration, autogenous bone grafting remains the gold standard for osseous reconstruction, with grafts typically harvested from intraoral or extraoral donor sites. These autografts are widely applied to restore defects in the craniofacial region due to their inherent biological properties.[138] However, the associated donor-site morbidity has led to the exploration of alternative grafting materials. An ideal graft material should demonstrate osteoconductive, osteoinductive, and osteogenic characteristics—criteria that are fully met only by autografts. Nevertheless, the invasiveness and complications linked to donor-site harvesting restrict their broader application. Consequently, a range of bone substitute materials have been introduced in the literature as potential alternatives, though they generally exhibit reduced regenerative potential compared to autologous grafts.[59,139-142]

Vivekanand et al. investigated the use of different bone substitute materials in the treatment of cystic bone defects, comparing bovine-derived hydroxyapatite (BHA) and synthetic hydroxyapatite (SHA) grafts. Their findings indicated that both materials were biocompatible and suitable for defect filling, exhibiting favorable outcomes in terms of reduced resorption and enhanced bone formation. The study concluded that BHA and SHA demonstrated comparable efficacy, supporting their use as viable alternatives to autologous grafts in specific clinical scenarios.[143]

Serum albumin has emerged as a key endogenous protein involved in the early stages of bone regeneration. Horváthy et al. investigated the attachment of stem cells to serum albumin-coated demineralized bone matrices using a rat calvarial defect model. Their findings demonstrated that bone defects treated with BoneAlbumin achieved complete union and the development of biomechanically functional new bone. These results highlight the regenerative potential of albumin-

coated graft materials and support their application in the clinical management of bone defects.[144,145]

Kivovics et al. hypothesized that albumin-coated allografts may promote superior bone remodeling compared to anorganic xenografts. Their comparative study, which included histological, histomorphometric, and microcomputed tomography (μCT) analyses, revealed that while anorganic bovine bone mineral was largely incorporated into newly formed bone, the BoneAlbumin grafts primarily underwent active remodeling processes. These findings suggest a dynamic integration pattern for albumin-coated allografts, supporting their potential utility in clinical bone regeneration strategies.[146]

Simonffy et al. also examined the regenerative potential of various bone graft materials, including BoneAlbumin. Their study aimed to compare the clinical outcomes of bovine xenograft (Bio-Oss) and BoneAlbumin in mandibular third molar extraction socket grafting, focusing on bone remodeling and the incidence of postoperative complications. The results indicated that BoneAlbumin use led to a greater degree of bone regeneration compared to native bone formation, xenograft application, or spontaneous healing of the socket without any grafting material.[147]

Evidence from the literature supports the effectiveness of serum albumin-coated bone allograft (BoneAlbumin) as a viable bone substitute, not only in maxillofacial surgery but also in orthopedic applications. Gyulay et al. demonstrated its long-term efficacy in orthopedic surgery, with favorable outcomes observed during a 7-year follow-up period.[148]

The effectiveness of platelet concentrates in enhancing wound healing and tissue regeneration remains a subject of debate in academic discourse. Platelet-rich fibrin (PRF) was first introduced by Choukroun et al. in 2006 as an adjunct to promote new bone formation in allografts and to shorten the healing period to four months

following maxillary sinus augmentation. PRF offers the potential to restore some of the osteoinductive properties diminished during the fabrication of bone-substitute materials by releasing autologous growth factors that promote accelerated bone remodeling. Furthermore, the adoption of a low-speed centrifugation protocol for the preparation of advanced PRF (A-PRF) has been shown to increase the concentration of growth factors within the scaffold and to extend its shelf life up to 14 days, thereby supporting its use in guided bone regeneration procedures.[15,19,149,150]

Further evidence supporting the combined use of A-PRF and BoneAlbumin has been provided by Trimmel et al., who investigated the microarchitectural characteristics of augmented bone following maxillary sinus augmentation. Their study compared healing outcomes after 3 months (test group) and 6 months (control group) using a composite graft of BoneAlbumin and A-PRF. The findings indicated that this combination allowed for successful bone regeneration even after a shortened healing period, effectively reducing the total treatment time by 3 months in a two-stage maxillary sinus augmentation protocol.[59]

5.3. Limitations

5.3.1. Limitations of the 3D Scanner Validation Study

The validation study comparing direct caliper measurements to 3D scanning was limited by a relatively small number of participants and the use of a volunteer population. Measurements were performed on live subjects, which introduces potential variability due to involuntary facial movements, soft tissue compression, and differences in facial expression especially in the perioral region. These factors can affect both direct and indirect measurements.[82,106]

Furthermore, the participation of both experienced and inexperienced examiners highlighted variability due to operator skill. Although most measurements showed

strong agreement and high correlation coefficients, significant differences were noted at specific points (e.g., subnasale–menton, cheilion–cheilion), particularly with the caliper method.[82]

The time required for image post-processing with the scanner, although decreasing with experience, represents a logistical limitation in fast-paced clinical workflows. Additionally, while the EINSTAR scanner showed promise, it was validated against manual caliper measurements rather than a photogrammetric gold standard (e.g., 3dMD or Vectra), which may limit direct comparisons with existing high-end systems.[82,86]

5.3.2. Limitations of the Randomized Controlled Trial

One of the primary limitations of this study is the small sample size (n = 20), which inherently reduces statistical power and may limit the ability to detect subtle differences between the groups. While the sample size is acceptable for a preliminary pilot study, the findings should be interpreted with appropriate caution. Confirmation through larger, adequately powered randomized controlled trials is necessary to validate these results and strengthen the generalizability of the observed effects. Furthermore, multiple statistical comparisons were performed without adjustment for multiplicity; therefore, the findings should be considered exploratory and interpreted with caution. [48,52]

Secondly, the short follow-up period of seven days limits the evaluation to early postoperative outcomes such as pain, swelling, and immediate quality-of-life measures. Important long-term parameters—including bone regeneration, soft-tissue stability, and sustained improvements in patient-reported outcomes—were not assessed. This shortcoming restricts the ability to draw conclusions about the prolonged clinical benefits of PRF. A volumetric follow-up study by Sharma et al. reported continued healing in a large periapical lesion over a two-year period when PRF was combined with a bone substitute, reinforcing the importance of extended

observation. Furthermore, previous evidence suggests that PRF may exert beneficial effects not only in the early healing phase but also over the long term, particularly when used adjunctively in surgical interventions.[55,151]

Thirdly, the study was conducted at a single academic institution under controlled clinical conditions and performed by a single surgeon. While this approach enhances internal validity by reducing procedural variability, it may limit the generalizability of the findings. In real-world settings, differences in operator skill, clinical protocols, PRF preparation techniques, and patient characteristics may influence treatment outcomes. As such, future multicenter studies are necessary to determine whether the observed benefits of PRF are consistent across diverse clinical environments and provider experience levels.[134,152]

Moreover, several potential sources of bias must be considered. The single-center design and the application of strict eligibility criteria may have introduced selection bias, thereby limiting the heterogeneity of the study population. Additionally, the single-blind design where only participants were blinded, while the operating surgeon remained aware of treatment allocation may have introduced performance bias. Although outcome assessments were conducted by an independent evaluator blinded to group assignment, the possibility of detection bias cannot be entirely excluded. These factors may have influenced the internal validity of the findings and highlight the importance of conducting future multicenter, double-blind randomized trials with broader inclusion criteria to improve both methodological rigor and external validity.[54]

Additionally, although validated instruments such as the PROMIS-29+2 Profile were employed to assess patient-reported outcomes, potential cultural and linguistic influences on questionnaire interpretation must be acknowledged. This is particularly relevant in light of Hungarian validation studies of the PROMIS framework, which suggest that localized adaptation may impact the perception of certain health domains. Furthermore, no preoperative platelet count was recorded,

which could have provided useful biological context regarding individual variability in PRF clot quality and regenerative potential. Inclusion of such data in future investigations may strengthen the biological interpretation of clinical outcomes.[132]

While encouraging, these findings are limited by these methodological constraints. Larger, multicenter, double-blind randomized controlled trials with extended follow-up periods are warranted to validate the observed benefits, assess long-term regenerative outcomes, and compare PRF with other autologous biomaterials such as platelet-rich plasma or advanced PRF variants.

5.3.3. Limitations of the Case Report (BoneAlbumin + A-PRF)

As a single-patient case study, the results presented regarding the composite use of A-PRF and BoneAlbumin are not generalizable. While µCT and histomorphometric analysis provided detailed insights into bone healing and graft behavior, no statistical analysis or comparison with a control group was possible.[57,59]

Although similarities were observed between 3-month and 6-month healing outcomes, these findings must be interpreted with caution. Individual healing capacity, lesion characteristics, and patient-specific anatomical or systemic factors may all influence results in a way that cannot be isolated in a single case.[57,135]

Additionally, the concurrent use of two biomaterials (BoneAlbumin and A-PRF) does not allow for clear attribution of the observed regenerative effect to one or the other. Future controlled studies comparing these materials individually and in combination are needed to validate the preliminary observations.[8,146]

5.4. Future Directions

Future research should explore the broader clinical and research potential of low-cost handheld 3D facial scanners, such as the EINSTAR device, in oral and maxillofacial surgery. Beyond basic anthropometric validation, this technology holds promise for application in preoperative planning, postoperative outcome evaluation, swelling assessment, cleft lip and craniofacial anomaly documentation, and longitudinal growth studies. Its portability, affordability, and user-friendliness make it particularly suitable for routine use in clinical settings and for data collection in larger-scale research projects. Further investigations should assess the scanner's accuracy in dynamic conditions, its reproducibility across time and operators, and its performance in patients with soft-tissue asymmetries or surgical alterations. The integration of automated landmark detection and AI-assisted analysis may further enhance its utility and reliability across diverse clinical scenarios.

Building upon the preliminary findings of this randomized pilot trial, future studies should aim to validate the clinical benefits of PRF membranes in periapical surgery through larger, multicenter, double-blind randomized controlled trials. These studies should incorporate longer follow-up periods to assess sustained soft-tissue healing, bone regeneration, and long-term quality-of-life improvements. Additionally, it would be valuable to investigate biological correlates such as individual platelet counts or clot characteristics, which may influence PRF efficacy. Comparative studies examining different PRF protocols (e.g., A-PRF, i-PRF, or AL-PRF) or the adjunctive use of occlusive barriers could provide deeper insight into the optimization of regenerative outcomes. Incorporating PROMIS-based patient-reported outcomes and volumetric facial analysis may help establish standardized, patient-centered endpoints for future surgical endodontic research.

Future investigations should further explore the regenerative capacity of BoneAlbumin and A-PRF composites in various clinical contexts, including larger

cystic lesions, post-traumatic defects, and sinus augmentations. Controlled clinical trials comparing this composite to other widely used grafting materials—such as xenografts or autografts—would provide more robust evidence regarding its efficacy and remodeling dynamics. Moreover, histological and radiological follow-up at standardized intervals could help clarify the timeline of bone formation and graft resorption. The application of this composite graft in patients with systemic conditions affecting bone metabolism (e.g., osteoporosis or diabetes) may also represent a promising area of investigation. Overall, further controlled clinical studies are needed to determine whether the combined use of serum albumin-coated allografts and autologous platelet concentrates can shorten healing time and improve clinical outcomes in oral and maxillofacial surgery.

6. Conclusion

This dissertation comprised three interconnected clinical investigations aimed at enhancing the accuracy of diagnostic methods, improving postoperative outcomes, and evaluating novel biomaterials in oral and maxillofacial surgery. Collectively, the findings provide further evidence regarding the potential clinical applications of digital technologies and biologically active materials in oral and maxillofacial surgery.

The first study validated the use of a handheld 3D facial scanner (EINSTAR) against conventional caliper measurements. The results demonstrated that 3D surface scanning provides accurate, reproducible, and clinically acceptable measurements of facial soft tissues. Although scanning and processing times were slightly longer, the ability to store, re-analyze, and digitally manipulate data offers significant advantages, particularly in research, treatment planning, and follow-up in maxillofacial surgery.

The second investigation, a pilot randomized controlled trial, showed that the adjunctive use of platelet-rich fibrin (PRF) membranes during apicoectomy was associated with lower early postoperative swelling and pain, as well as more favorable quality-of-life outcomes. These results suggest that PRF may improve early postoperative recovery and patient comfort, supporting its potential as an adjunctive autologous biomaterial in periapical surgery. Though preliminary, these findings provide a strong rationale for further multicenter trials to evaluate long-term outcomes and generalizability.

The third case-based study evaluated the composite use of A-PRF and BoneAlbumin in a patient with Gorlin–Goltz syndrome undergoing multiple cystectomies. Histological and radiological findings demonstrated bone remodeling in the augmented areas, with successful implant placement performed after a shortened healing period. These preliminary observations support further controlled

investigation of this composite graft approach in bone regeneration following cystectomy.

In summary, the studies presented herein provide further evidence regarding the clinical applications of digital diagnostics, patient-reported outcome measures, and regenerative biomaterials in oral and maxillofacial surgery. Together, they contribute to the growing body of evidence supporting patient-centered, technology-assisted, and biologically guided approaches in this field.

7. Summary

The present doctoral dissertation provides a multidimensional investigation into novel diagnostic and therapeutic modalities that support tissue regeneration and improve clinical outcomes in oral and maxillofacial surgery.

The first study confirmed the reliability and clinical applicability of the EINSTAR 3D scanner for facial soft tissue assessment. The scanner showed high measurement consistency and clinically acceptable accuracy, while its non-invasive digital workflow makes it a valuable tool for diagnosis and postoperative follow-up in oral and maxillofacial surgery.

The second study, a randomized controlled clinical trial, evaluated the effect of platelet-rich fibrin (PRF) membranes on postoperative recovery after apicoectomy. PRF significantly reduced postoperative pain and facial swelling, assessed by 3D surface imaging, and improved short-term quality of life measured with the PROMIS-29+2 Profile. These findings suggest a potential beneficial effect of PRF on early postoperative recovery and support its further investigation as an adjunct in periapical surgery.

The third study describes the use of a composite graft consisting of albumin-coated bone allograft (BoneAlbumin) and advanced PRF (A-PRF) following multiple cystectomies in a patient with Gorlin–Goltz syndrome. Micro-CT and histomorphometric analyses documented bone remodeling in the augmented areas at three and six months, providing preliminary observations on the healing characteristics of the composite graft.

Together, these studies support the clinical potential of regenerative biomaterials and digital imaging in oral and maxillofacial surgery. Further large-scale studies are needed to confirm these findings and optimize clinical protocols.

8. References

1. Toma, A.I.; Fuller, J.M.; Willett, N.J.; Goudy, S.L. Oral wound healing models and emerging regenerative therapies. *Transl Res* **2021**, *236*, 17–34, doi:10.1016/j.trsl.2021.06.003.
2. Dohan, D.M.; Choukroun, J.; Diss, A.; Dohan, S.L.; Dohan, A.J.; Mouhyi, J.; Gogly, B. Platelet-rich fibrin (PRF): a second-generation platelet concentrate. Part II: platelet-related biologic features. *Oral Surg Oral Med Oral Pathol Oral Radiol Endod* **2006**, *101*, e45–e50, doi:10.1016/j.tripleo.2005.07.009.
3. Dohan, D.M.; Choukroun, J.; Diss, A.; Dohan, S.L.; Dohan, A.J.; Mouhyi, J.; Gogly, B. Platelet-rich fibrin (PRF): a second-generation platelet concentrate. Part III: leucocyte activation: a new feature for platelet concentrates? *Oral Surg Oral Med Oral Pathol Oral Radiol Endod* **2006**, *101*, e51–e55, doi:10.1016/j.tripleo.2005.07.010.
4. Burnham, A.J.; Toma, A.I.; Shah, D.; Cha, T.; Kaimari, S.; Behara, M.; Sekar, K.P.C.; Kamalakar, A.; Willett, N.; Botchwey, E.; et al. FTY720P-treated macrophages in PEG-4MAL hydrogels promote oral wound healing. *Cytotherapy* **2025**, *27*, 338–349, doi:10.1016/j.jcyt.2024.11.002.
5. Politis, C.; Schoenaers, J.; Jacobs, R.; Agbaje, J.O. Wound Healing Problems in the Mouth. *Front Physiol* **2016**, *7*, 507, doi:10.3389/fphys.2016.00507.
6. Koh, T.J.; DiPietro, L.A. Inflammation and wound healing: the role of the macrophage. *Expert Rev Mol Med* **2011**, *13*, e23, doi:10.1017/S1462399411001943.
7. Cho, S.K.; Mattke, S.; Gordon, H.; Sheridan, M.; Ennis, W. Development of a Model to Predict Healing of Chronic Wounds Within 12 Weeks. *Adv Wound Care (New Rochelle)* **2020**, *9*, 516–524, doi:10.1089/wound.2019.1091.
8. Fan, Y.; Perez, K.; Dym, H. Clinical uses of platelet-rich fibrin in oral and maxillofacial surgery. *Dent Clin North Am* **2020**, *64*, 291–303, doi:10.1016/j.cden.2019.12.012.
9. Kingsley, C.S. Blood coagulation; evidence of an antagonist to factor VI in platelet-rich human plasma. *Nature* **1954**, *173*, 723–724, doi:10.1038/173723a0.

10. Alves, R.; Grimalt, R. A Review of Platelet-Rich Plasma: History, Biology, Mechanism of Action, and Classification. *Skin Appendage Disord* **2018**, *4*, 18–24, doi:10.1159/000477353.
11. Egierska, D.; Perszke, M.; Mazur, M.; Dus-Ilnicka, I. Platelet-rich plasma and platelet-rich fibrin in oral surgery: A narrative review. *Dent Med Probl* **2023**, *60*, 177–186, doi:10.17219/dmp/147298.
12. Matras, H. [Effect of various fibrin preparations on reimplantations in the rat skin]. *Osterr Z Stomatol* **1970**, *67*, 338–359.
13. Agrawal, A.A. Evolution, current status and advances in application of platelet concentrate in periodontics and implantology. *World J Clin Cases* **2017**, *5*, 159–171, doi:10.12998/wjcc.v5.i5.159.
14. Marx, R.E.; Carlson, E.R.; Eichstaedt, R.M.; Schimmele, S.R.; Strauss, J.E.; Georgeff, K.R. Platelet-rich plasma: Growth factor enhancement for bone grafts. *Oral Surg Oral Med Oral Pathol Oral Radiol Endod* **1998**, *85*, 638–646, doi:10.1016/s1079-2104(98)90029-4.
15. Choukroun J, A.F., Schoffler C, Vervelle A. Une opportunite' en paro-implantologie: le PRF. *Implantodontie* **2000**, *42*, 55–62.
16. Dohan, D.M.; Choukroun, J.; Diss, A.; Dohan, S.L.; Dohan, A.J.; Mouhyi, J.; Gogly, B. Platelet-rich fibrin (PRF): a second-generation platelet concentrate. Part I: technological concepts and evolution. *Oral Surg Oral Med Oral Pathol Oral Radiol Endod* **2006**, *101*, e37–e44, doi:10.1016/j.tripleo.2005.07.008.
17. Ghanaati, S.; Booms, P.; Orlowska, A.; Kubesch, A.; Lorenz, J.; Rutkowski, J.; Landes, C.; Sader, R.; Kirkpatrick, C.; Choukroun, J. Advanced platelet-rich fibrin: a new concept for cell-based tissue engineering by means of inflammatory cells. *J Oral Implantol* **2014**, *40*, 679–689, doi:10.1563/aaid-joi-D-14-00138.
18. Liu, Y.; Sun, X.; Yu, J.; Wang, J.; Zhai, P.; Chen, S.; Liu, M.; Zhou, Y. Platelet-rich fibrin as a bone graft material in oral and maxillofacial bone regeneration: classification and summary for better application. *Biomed Res Int* **2019**, *2019*, 3295756, doi:10.1155/2019/3295756.

19. Miron, R.J.; Zucchelli, G.; Pikos, M.A.; Salama, M.; Lee, S.; Guillemette, V.; Fujioka-Kobayashi, M.; Bishara, M.; Zhang, Y.; Wang, H.L.; et al. Use of platelet-rich fibrin in regenerative dentistry: a systematic review. *Clin Oral Investig* **2017**, *21*, 1913–1927, doi:10.1007/s00784-017-2133-z.
20. Baaten, C.; Nagy, M.; Bergmeier, W.; Spronk, H.M.H.; van der Meijden, P.E.J. Platelet biology and function: plaque erosion vs. rupture. *Eur Heart J* **2024**, *45*, 18–31, doi:10.1093/eurheartj/ehad720.
21. Smith, C.W. Release of alpha-granule contents during platelet activation. *Platelets* **2022**, *33*, 491–502, doi:10.1080/09537104.2021.1913576.
22. Dohan Ehrenfest, D.M.; Pinto, N.R.; Pereda, A.; Jimenez, P.; Corso, M.D.; Kang, B.S.; Nally, M.; Lanata, N.; Wang, H.L.; Quirynen, M. The impact of the centrifuge characteristics and centrifugation protocols on the cells, growth factors, and fibrin architecture of a leukocyte- and platelet-rich fibrin (L-PRF) clot and membrane. *Platelets* **2018**, *29*, 171–184, doi:10.1080/09537104.2017.1293812.
23. Schilephake, H. Bone growth factors in maxillofacial skeletal reconstruction. *Int J Oral Maxillofac Surg* **2002**, *31*, 469–484, doi:10.1054/ijom.2002.0244.
24. Deng, Z.; Fan, T.; Xiao, C.; Tian, H.; Zheng, Y.; Li, C.; He, J. TGF-beta signaling in health, disease, and therapeutics. *Signal Transduct Target Ther* **2024**, *9*, 61, doi:10.1038/s41392-024-01764-w.
25. Hu, H.H.; Chen, D.Q.; Wang, Y.N.; Feng, Y.L.; Cao, G.; Vaziri, N.D.; Zhao, Y.Y. New insights into TGF-beta/Smad signaling in tissue fibrosis. *Chem Biol Interact* **2018**, *292*, 76–83, doi:10.1016/j.cbi.2018.07.008.
26. Amable, P.R.; Carias, R.B.; Teixeira, M.V.; da Cruz Pacheco, I.; Correa do Amaral, R.J.; Granjeiro, J.M.; Borojevic, R. Platelet-rich plasma preparation for regenerative medicine: optimization and quantification of cytokines and growth factors. *Stem Cell Res Ther* **2013**, *4*, 67, doi:10.1186/scrt218.
27. Solakoglu, O.; Heydecke, G.; Amiri, N.; Anitua, E. The use of plasma rich in growth factors (PRGF) in guided tissue regeneration and guided bone regeneration. A review of histological, immunohistochemical, histomorphometrical, radiological

and clinical results in humans. *Ann Anat* **2020**, *231*, 151528, doi:10.1016/j.aanat.2020.151528.

28. Dragonas, P.; Schiavo, J.H.; Avila-Ortiz, G.; Palaiologou, A.; Katsaros, T. Plasma rich in growth factors (PRGF) in intraoral bone grafting procedures: A systematic review. *J Craniomaxillofac Surg* **2019**, *47*, 443–453, doi:10.1016/j.jcms.2019.01.012.
29. LeRoith, D.; Holly, J.M.P.; Forbes, B.E. Insulin-like growth factors: Ligands, binding proteins, and receptors. *Mol Metab* **2021**, *52*, 101245, doi:10.1016/j.molmet.2021.101245.
30. Cecerska-Heryc, E.; Goszka, M.; Serwin, N.; Roszak, M.; Grygorcewicz, B.; Heryc, R.; Dolegowska, B. Applications of the regenerative capacity of platelets in modern medicine. *Cytokine Growth Factor Rev* **2022**, *64*, 84–94, doi:10.1016/j.cytogfr.2021.11.003.
31. Zwittnig, K.; Kirnbauer, B.; Jakse, N.; Schlenke, P.; Mischak, I.; Ghanaati, S.; Al-Maawi, S.; Vegh, D.; Payer, M.; Zrnc, T.A. Growth Factor Release within Liquid and Solid PRF. *J Clin Med* **2022**, *11*, doi:10.3390/jcm11175070.
32. Breen, E.C. VEGF in biological control. *J Cell Biochem* **2007**, *102*, 1358–1367, doi:10.1002/jcb.21579.
33. Liu, Y.H.; To, M.; Okudera, T.; Wada-Takahashi, S.; Takahashi, S.S.; Su, C.Y.; Matsuo, M. Advanced platelet-rich fibrin (A-PRF) has an impact on the initial healing of gingival regeneration after tooth extraction. *J Oral Biosci* **2022**, *64*, 141–147, doi:10.1016/j.job.2021.11.001.
34. Bielecki, T.; Dohan Ehrenfest, D.M.; Everts, P.A.; Wiczkowski, A. The role of leukocytes from L-PRP/L-PRF in wound healing and immune defense: new perspectives. *Curr Pharm Biotechnol* **2012**, *13*, 1153–1162, doi:10.2174/138920112800624373.
35. Song, P.; He, D.; Ren, S.; Fan, L.; Sun, J. Platelet-rich fibrin in dentistry. *J Appl Biomater Funct Mater* **2024**, *22*, 22808000241299588, doi:10.1177/22808000241299588.

36. Chmielewski, M.; Pilloni, A.; Adamska, P. Advanced Platelet-Rich Fibrin Plus (A-PRF+) as an Additive to Hard Tissue Managing Protocols in Oral Surgery: A Systematic Review. *J Funct Biomater* **2025**, *16*, doi:10.3390/jfb16040145.
37. Pereira, V.B.S.; Lago, C.A.P.; Almeida, R.A.C.; Barbirato, D.D.S.; Vasconcelos, B. Biological and Cellular Properties of Advanced Platelet-Rich Fibrin (A-PRF) Compared to Other Platelet Concentrates: Systematic Review and Meta-Analysis. *Int J Mol Sci* **2023**, *25*, doi:10.3390/ijms25010482.
38. Quirynen, M.; Blanco, J.; Wang, H.L.; Donos, N.; Temmerman, A.; Castro, A.; Pinto, N. Instructions for the use of L-PRF in different clinical indications. *Periodontol 2000* **2025**, *97*, 420–432, doi:10.1111/prd.12564.
39. Deterville, L.; Lasserre, J.F.; Toma, S. A prospective evaluation of subgingival irrigation with i-PRF following non-surgical treatment of peri-implantitis. *Front Dent Med* **2025**, *6*, 1568889, doi:10.3389/fdmed.2025.1568889.
40. Yasar, N.C.; Unsal, G.; Kocaelli, H.A.; Orhan, K.; Sag, F.B. Comparative Analysis of Local Application of Titanium-Platelet Rich Fibrin (T-PRF) and Leukocyte-Platelet Rich Fibrin (L-PRF) in Bone Defect Healing: A Micro-CT and Histopathological Study in Rabbit Models. *Microsc Res Tech* **2025**, *88*, 2073–2084, doi:10.1002/jemt.24841.
41. Shen, F.; Chai, J.; Wei, M.; Qian, X.; Shen, M. Next-generation platelet concentrate: Alb-PRF outperformed PRP and H-PRF in promoting endothelial function and wound healing. *Sci Rep* **2026**, *16*, doi:10.1038/s41598-026-44659-2.
42. Fujioka-Kobayashi, M.; Katagiri, H.; Kono, M.; Schaller, B.; Zhang, Y.; Sculean, A.; Miron, R.J. Improved growth factor delivery and cellular activity using concentrated platelet-rich fibrin (C-PRF) when compared with traditional injectable (i-PRF) protocols. *Clin Oral Investig* **2020**, *24*, 4373–4383, doi:10.1007/s00784-020-03303-7.
43. Yilmaz, M.F.; Omezli, M.M.; Torul, D.; Miron, R.J. Efficacy of injectable platelet-rich fibrin and concentrated platelet-rich fibrin injections combined with arthrocentesis in the management of temporomandibular joint internal disorders:

Randomized clinical trial. *J Craniomaxillofac Surg* **2026**, *54*, 104447, doi:10.1016/j.jcms.2026.104447.

44. Niemczyk, W.; Zurek, J.; Niemczyk, S.; Kepa, M.; Zieba, N.; Misiolek, M.; Wiench, R. Antibiotic-Loaded Platelet-Rich Fibrin (AL-PRF) as a New Carrier for Antimicrobials: A Systematic Review of In Vitro Studies. *Int J Mol Sci* **2025**, *26*, doi:10.3390/ijms26052140.
45. Malamed, S.F. Pain management following dental trauma and surgical procedures. *Dent Traumatol* **2023**, *39*, 295–303, doi:10.1111/edt.12840.
46. Lieblich, S.E. Current concepts of periapical surgery: 2020 update. *Oral Maxillofac Surg Clin North Am* **2020**, *32*, 571–582, doi:10.1016/j.coms.2020.07.007.
47. Canellas, J.; Medeiros, P.J.D.; Figueredo, C.; Fischer, R.G.; Ritto, F.G. Platelet-rich fibrin in oral surgical procedures: a systematic review and meta-analysis. *Int J Oral Maxillofac Surg* **2019**, *48*, 395–414, doi:10.1016/j.ijom.2018.07.007.
48. Sinha, A.; Jain, A.K.; Rao, R.D.; Sivasailam, S.; Jain, R. Effect of platelet-rich fibrin on periapical healing and resolution of clinical symptoms in patients following periapical surgery: A systematic review and meta-analysis. *J Conserv Dent Endod* **2023**, *26*, 366–376, doi:10.4103/jcd.jcd_195_23.
49. Singh, S.; Singh, A.; Singh, S.; Singh, R. Application of PRF in surgical management of periapical lesions. *Natl J Maxillofac Surg* **2013**, *4*, 94–99, doi:10.4103/0975-5950.117825.
50. Singh, S.; Swain, J.R.; Gugnani, M.; Arya, A.; Baghel, R.S.; Shafique, S. Periapical healing in endodontic retreatment: A comparative study of nano-hydroxyapatite with and without PRF. *Bioinformation* **2025**, *21*, 1195–1200, doi:10.6026/973206300211195.
51. Estrin, N.E.; Tran, T.B.; Ahmad, P.; Farshidfar, N.; Romanos, G.E.; Sculean, A.; Miron, R.J. Analgesic effects of platelet-rich fibrin (PRF): A systematic review. *Periodontol 2000* **2025**, doi:10.1111/prd.70014.
52. Soto-Penaloza, D.; Penarrocha-Diago, M.; Cervera-Ballester, J.; Penarrocha-Diago, M.; Tarazona-Alvarez, B.; Penarrocha-Oltra, D. Pain and quality of life after endodontic surgery with or without advanced platelet-rich fibrin membrane

application: a randomized clinical trial. *Clin Oral Investig* **2020**, *24*, 1727–1738, doi:10.1007/s00784-019-03033-5.

53. Zhu, J.; Zhang, S.; Yuan, X.; He, T.; Liu, H.; Wang, J.; Xu, B. Effect of platelet-rich fibrin on the control of alveolar osteitis, pain, trismus, soft tissue healing, and swelling following mandibular third molar surgery: an updated systematic review and meta-analysis. *Int J Oral Maxillofac Surg* **2021**, *50*, 398–406, doi:10.1016/j.ijom.2020.08.014.
54. Major, M.; Polyák, M.; Würsching, T.; Kammerhofer, G.; Kocsis, É.; Németh, Z.; Szabó, G. PRF Membranes Enhance Postoperative Recovery After Periapical Surgery: A Single-Blind Randomized Pilot Trial Using 3D Imaging. *Oral* **2025**, *5*, 98.
55. Al-Hamed, F.S.; Tawfik, M.A.; Abdelfadil, E.; Al-Saleh, M.A.Q. Efficacy of platelet-rich fibrin after mandibular third molar extraction: a systematic review and meta-analysis. *J Oral Maxillofac Surg* **2017**, *75*, 1124–1135, doi:10.1016/j.joms.2017.01.022.
56. Praganta, J.; De Silva, H.; De Silva, R.; Tong, D.C.; Thomson, W.M. Effect of advanced platelet-rich fibrin (A-PRF) on postoperative level of pain and swelling following third molar surgery. *J Oral Maxillofac Surg* **2024**, *82*, 581–589, doi:10.1016/j.joms.2024.02.003.
57. Major, M.; Kivovics, M.; Szabo, B.T.; Deri, T.; Polyak, M.; Jakob, N.P.; Csete, D.; Mocsai, A.; Nemeth, Z.; Szabo, G. Surgical Treatment of Multiple Bone Cysts Using a Platelet-Rich Fibrin and BoneAlbumin Composite Graft: A Case Report. *Reports (MDPI)* **2024**, *7*, doi:10.3390/reports7010007.
58. Yang, Z.; Zhai, S.; Liu, Y.; Wu, Y.; He, T.; Shi, X.; Chu, S. Sticky Bone: Advances and Applications. *Int J Nanomedicine* **2025**, *20*, 10151–10175, doi:10.2147/IJN.S524115.
59. Trimmel, B.; Gyulai-Gaal, S.; Kivovics, M.; Jakob, N.P.; Hegedus, C.; Szabo, B.T.; Dobo-Nagy, C.; Szabo, G. Evaluation of the Histomorphometric and Micromorphometric Performance of a Serum Albumin-Coated Bone Allograft Combined with A-PRF for Early and Conventional Healing Protocols after

Maxillary Sinus Augmentation: A Randomized Clinical Trial. *Materials (Basel)* **2021**, *14*, doi:10.3390/ma14071810.

60. Serafini, G.; Lollobrigida, M.; Fortunato, L.; Mazzucchi, G.; Lamazza, L.; Di Nardo, D.; Vozza, I.; Riminucci, M.; De Biase, A. Postextractive Alveolar Ridge Preservation Using L-PRF: Clinical and Histological Evaluation. *Case Rep Dent* **2020**, *2020*, 5073519, doi:10.1155/2020/5073519.
61. Shetty, N.R.; Menaka, K.B. Effect of platelet concentrates on the treatment outcome of peri implantitis: A systematic review. *J Indian Soc Periodontol* **2023**, *27*, 140–145, doi:10.4103/jisp.jisp_622_21.
62. Canullo, L.; Del Fabbro, M.; Khijmatgar, S.; Panda, S.; Ravida, A.; Tommasato, G.; Sculean, A.; Pesce, P. Dimensional and histomorphometric evaluation of biomaterials used for alveolar ridge preservation: a systematic review and network meta-analysis. *Clin Oral Investig* **2022**, *26*, 141–158, doi:10.1007/s00784-021-04248-1.
63. Al-Mahdi, A.H.; Abdulrahman, M.S.; Al-Jumaily, H.A.H. Evaluation of the Effectiveness of Using Platelet Rich Fibrin (PRF) With Bone Graft in the Reconstruction of Alveolar Cleft, A Prospective Study. *J Craniofac Surg* **2021**, *32*, 2139–2143, doi:10.1097/SCS.0000000000007486.
64. Malcangi, G.; Patano, A.; Palmieri, G.; Di Pede, C.; Latini, G.; Inchingolo, A.D.; Hazballa, D.; de Ruvo, E.; Garofoli, G.; Inchingolo, F.; et al. Maxillary Sinus Augmentation Using Autologous Platelet Concentrates (Platelet-Rich Plasma, Platelet-Rich Fibrin, and Concentrated Growth Factor) Combined with Bone Graft: A Systematic Review. *Cells* **2023**, *12*, doi:10.3390/cells12131797.
65. Trimmel, B.; Gede, N.; Hegyi, P.; Szakacs, Z.; Mezey, G.A.; Varga, E.; Kivovics, M.; Hanak, L.; Rumbus, Z.; Szabo, G. Relative performance of various biomaterials used for maxillary sinus augmentation: A Bayesian network meta-analysis. *Clin Oral Implants Res* **2021**, *32*, 135–153, doi:10.1111/clr.13690.
66. Mubarak, R.; Adel-Khattab, D.; Abdel-Ghaffar, K.A.; Gamal, A.Y. Adjunctive effect of collagen membrane coverage to L-PRF in the treatment of periodontal

intrabony defects: a randomized controlled clinical trial with biochemical assessment. *BMC Oral Health* **2023**, *23*, 631.

67. Miron, R.J.; Moraschini, V.; Fujioka-Kobayashi, M.; Zhang, Y.; Kawase, T.; Cosgarea, R.; Jepsen, S.; Bishara, M.; Canullo, L.; Shirakata, Y.; et al. Use of platelet-rich fibrin for the treatment of periodontal intrabony defects: a systematic review and meta-analysis. *Clin Oral Investig* **2021**, *25*, 2461–2478, doi:10.1007/s00784-021-03825-8.
68. Shokry, M.; Melek, L.N.F.; Amer, T.A. Three-dimensional volumetric analysis of bone regeneration following jaw cyst enucleation with and without an autologous albumin gel-platelet-rich fibrin mixture (Alb-PRF): a randomized controlled clinical trial. *BMC Oral Health* **2025**, *25*, 693, doi:10.1186/s12903-025-06027-w.
69. Garcia, J.C.; Guevara, H.A.; Crimi, S.; Minervini, G.; Manresa, C.; Gonzalez, M.D.; Malave, L.; Cicciu, M.; Millan-Golindano, C.F. Clinical behavior of bone regeneration therapy with platelet-rich fibrin in cystic cavities: a systematic review. *Minerva Dent Oral Sci* **2025**, doi:10.23736/S2724-6329.25.04876-4.
70. Oliva, S.; Lorusso, F.; Scarano, A.; D'Amario, M.; Murmura, G. The Treatment and Management of Oroantral Communications and Fistulas: A Systematic Review and Network Metanalysis. *Dent J (Basel)* **2024**, *12*, doi:10.3390/dj12050147.
71. Jung, J.W.; Hong, S.O.; Lee, E.J.; Kim, R.Y.; Jee, Y.J. The double-barrier technique using platelet-rich fibrin for closure of oroantral fistulas. *J Korean Assoc Oral Maxillofac Surg* **2023**, *49*, 163–168, doi:10.5125/jkaoms.2023.49.3.163.
72. Azadi, A.; Rezaei, F.; Yazdani, A.; Hejazi, K.; Moallem Savasari, A.; Amid, R.; Kadkhodazadeh, M. Hard and soft tissue alterations after the application of different soft tissue grafting materials during immediate dental implant placement: a systematic review and Bayesian network meta-analysis. *BMC Oral Health* **2025**, *25*, 183, doi:10.1186/s12903-025-05461-0.
73. Bhagwat, P.; Kamat, R.; Rao, P.; Ashok, K.; Shitole, P.; Sachdev, S.S. Evaluation of Root Coverage in Gingival Recessions Treated With Collagen Matrix and Platelet-Rich Fibrin: A Systematic Review. *Cureus* **2025**, *17*, e97385, doi:10.7759/cureus.97385.

74. Omidkhoda, M.; Jahnabin, A.; Khoshandam, F.; Eslami, F.; Hosseini Zarch, S.H.; Tavakol Afshari, J.; Kermani, H. Efficacy of Platelet-Rich Fibrin Combined with Autogenous Bone Graft in the Quality and Quantity of Maxillary Alveolar Cleft Reconstruction. *Iran J Otorhinolaryngol* **2018**, *30*, 329–334.
75. Nemeth, Z.; Bogdan, S.; Joob-Fancsaly, A.; Vaszilko, M.; Toth, A.; Szentpeteri, S. [Medication-related osteonecrosis of the jaw (MRONJ) during the treatment of cancer patients]. *Magy Onkol* **2025**, *69*, 118–127.
76. Jiang, A.; Zhang, Z.; Qiu, X.; Guo, Q. Medication-related osteonecrosis of the jaw (MRONJ): a review of pathogenesis hypothesis and therapy strategies. *Arch Toxicol* **2024**, *98*, 689–708, doi:10.1007/s00204-023-03653-7.
77. Szentpeteri, S.; Schmidt, L.; Restar, L.; Csaki, G.; Szabo, G.; Vaszilko, M. The effect of platelet-rich fibrin membrane in surgical therapy of medication-related osteonecrosis of the jaw. *J Oral Maxillofac Surg* **2020**, *78*, 738–748, doi:10.1016/j.joms.2019.12.008.
78. Arshad, S.; Tehreem, F.; Rehab Khan, M.; Ahmed, F.; Marya, A.; Karobari, M.I. Platelet-Rich Fibrin Used in Regenerative Endodontics and Dentistry: Current Uses, Limitations, and Future Recommendations for Application. *Int J Dent* **2021**, *2021*, 4514598, doi:10.1155/2021/4514598.
79. Hasanzade, T.; Ertugrul, A.S.; Yuzbasioglu Ertugrul, B. Effects of Injectable Platelet-Rich Fibrin on the Osseointegration of Dental Implants. *Med Sci Monit* **2025**, *31*, e949298, doi:10.12659/MSM.949298.
80. Tommasato, G.; Del Fabbro, M.; Oliva, N.; Khijmatgar, S.; Grusovin, M.G.; Sculean, A.; Canullo, L. Autogenous graft versus collagen matrices for peri-implant soft tissue augmentation. A systematic review and network meta-analysis. *Clin Oral Investig* **2024**, *28*, 300, doi:10.1007/s00784-024-05684-5.
81. Nagori, S.A.; Gopalakrishnan, V.; Rangarajan, H.; Kulkarni, V.; Roychoudhury, A. Does intra-articular injection of platelet-rich plasma/platelet-rich fibrin improve outcomes after temporomandibular joint arthrocentesis? A systematic review and meta-analysis. *Br J Oral Maxillofac Surg* **2024**, *62*, 676–684, doi:10.1016/j.bjoms.2024.06.007.

82. Major, M.; Meszaros, B.; Wursching, T.; Polyak, M.; Kammerhofer, G.; Nemeth, Z.; Szabo, G.; Nagy, K. Evaluation of a structured light scanner for 3D facial imaging: a comparative study with direct anthropometry. *Sensors (Basel)* **2024**, *24*, 5286, doi:10.3390/s24165286.

83. Wersenyi, G.; Scheper, V.; Spagnol, S.; Eixelberger, T.; Wittenberg, T. Cost-effective 3D scanning and printing technologies for outer ear reconstruction: current status. *Head Face Med* **2023**, *19*, 46, doi:10.1186/s13005-023-00394-x.

84. Liberton, D.K.; Mishra, R.; Beach, M.; Raznahan, A.; Gahl, W.A.; Manoli, I.; Lee, J.S. Comparison of Three-Dimensional Surface Imaging Systems Using Landmark Analysis. *J Craniofac Surg* **2019**, *30*, 1869–1872, doi:10.1097/SCS.0000000000005795.

85. Hollander, M.H.J.; Kraeima, J.; Meesters, A.M.L.; Delli, K.; Vissink, A.; Jansma, J.; Schepers, R.H. Reproducibility of 3D scanning in the periorbital region. *Sci Rep* **2021**, *11*, 3671, doi:10.1038/s41598-021-83335-5.

86. Camison, L.; Bykowski, M.; Lee, W.W.; Carlson, J.C.; Roosenboom, J.; Goldstein, J.A.; Losee, J.E.; Weinberg, S.M. Validation of the Vectra H1 portable three-dimensional photogrammetry system for facial imaging. *Int J Oral Maxillofac Surg* **2018**, *47*, 403–410, doi:10.1016/j.ijom.2017.08.008.

87. de Menezes, M.; Rosati, R.; Ferrario, V.F.; Sforza, C. Accuracy and reproducibility of a 3-dimensional stereophotogrammetric imaging system. *J Oral Maxillofac Surg* **2010**, *68*, 2129–2135, doi:10.1016/j.joms.2009.09.036.

88. Ayoub, A.; Khan, A.; Aldhanhani, A.; Alnaser, H.; Naudi, K.; Ju, X.; Gillgrass, T.; Mossey, P. The Validation of an Innovative Method for 3D Capture and Analysis of the Nasolabial Region in Cleft Cases. *Cleft Palate Craniofac J* **2021**, *58*, 98–104, doi:10.1177/1055665620946987.

89. Gallardo, Y.N.R.; Salazar-Gamarra, R.; Bohner, L.; De Oliveira, J.I.; Dib, L.L.; Sesma, N. Evaluation of the 3D error of 2 face-scanning systems: An in vitro analysis. *J Prosthet Dent* **2023**, *129*, 630–636, doi:10.1016/j.prosdent.2021.06.049.

90. Zhou, S.; Xiao, S. 3D face recognition: a survey. *Human-centric Computing and Information Sciences* **2018**, *8*, 35.

91. Li, M.; Huang, B.; Tian, G. A comprehensive survey on 3D face recognition methods. *Engineering Applications of Artificial Intelligence* **2022**, *110*, 104669.
92. Shamata, A.; Thompson, T. Documentation and analysis of traumatic injuries in clinical forensic medicine involving structured light three-dimensional surface scanning versus photography. *Journal of forensic and legal medicine* **2018**, *58*, 93–100.
93. Maiese, A.; Manetti, A.C.; Ciallella, C.; Fineschi, V. The introduction of a new diagnostic tool in forensic pathology: LiDAR sensor for 3D autopsy documentation. *Biosensors* **2022**, *12*, 132.
94. Franco de Sa Gomes, C.; Libdy, M.R.; Normando, D. Scan time, reliability and accuracy of craniofacial measurements using a 3D light scanner. *J Oral Biol Craniofac Res* **2019**, *9*, 331–335, doi:10.1016/j.jobcr.2019.07.001.
95. Ferrario, V.F.; Sforza, C.; Dellavia, C.; Tartaglia, G.M.; Colombo, A.; Carù, A. A quantitative three-dimensional assessment of soft tissue facial asymmetry of cleft lip and palate adult patients. *Journal of Craniofacial Surgery* **2003**, *14*, 739–746.
96. Modabber, A.; Peters, F.; Kniha, K.; Goloborodko, E.; Ghassemi, A.; Lethaus, B.; Holzle, F.; Mohlhenrich, S.C. Evaluation of the accuracy of a mobile and a stationary system for three-dimensional facial scanning. *J Craniomaxillofac Surg* **2016**, *44*, 1719–1724, doi:10.1016/j.jcms.2016.08.008.
97. Ye, H.; Lv, L.; Liu, Y.; Zhou, Y. Evaluation of the Accuracy, Reliability, and Reproducibility of Two Different 3D Face-Scanning Systems. *The International journal of prosthodontics* **2016**, *29*, 213–218.
98. Weinberg, S.M.; Scott, N.M.; Neiswanger, K.; Brandon, C.A.; Marazita, M.L. Digital three-dimensional photogrammetry: evaluation of anthropometric precision and accuracy using a Genex 3D camera system. *The Cleft palate-craniofacial journal* **2004**, *41*, 507–518.
99. Andrade, L.M.; da Silva, A.M.B.R.; Magri, L.V.; da Silva, M.A.M.R. Repeatability study of angular and linear measurements on facial morphology analysis by means of stereophotogrammetry. *Journal of Craniofacial Surgery* **2017**, *28*, 1107–1111.

100. Tzou, C.-H.J.; Frey, M. Evolution of 3D surface imaging systems in facial plastic surgery. *Facial Plastic Surgery Clinics* **2011**, *19*, 591–602.

101. Akan, B.; Akan, E.; Sahan, A.O.; Kalak, M. Evaluation of 3D Face-Scan images obtained by stereophotogrammetry and smartphone camera. *Int Orthod* **2021**, *19*, 669–678, doi:10.1016/j.ortho.2021.08.007.

102. Weinberg, S.M.; Kolar, J.C. Three-dimensional surface imaging: limitations and considerations from the anthropometric perspective. *J Craniofac Surg* **2005**, *16*, 847–851, doi:10.1097/01.scs.0000164330.96675.0c.

103. Modabber, A.; Rana, M.; Ghassemi, A.; Gerressen, M.; Gellrich, N.C.; Holzle, F.; Rana, M. Three-dimensional evaluation of postoperative swelling in treatment of zygomatic bone fractures using two different cooling therapy methods: a randomized, observer-blind, prospective study. *Trials* **2013**, *14*, 238, doi:10.1186/1745-6215-14-238.

104. Mai, H.N.; Lee, D.H. Accuracy of Mobile Device-Compatible 3D Scanners for Facial Digitization: Systematic Review and Meta-Analysis. *J Med Internet Res* **2020**, *22*, e22228, doi:10.2196/22228.

105. Sforza, C.; de Menezes, M.; Ferrario, V. Soft- and hard-tissue facial anthropometry in three dimensions: what's new. *J Anthropol Sci* **2013**, *91*, 159–184, doi:10.4436/jass.91007.

106. Nogueira, B.R.; Oliveira Junior, O.B.; de Sousa Gomes Costa, J.L.; Zanetti, T.F.; Pretel, H. Cloner 3D photogrammetric facial scanner: Assessment of accuracy in a controlled clinical study. *J Esthet Restor Dent* **2023**, *35*, 508–516, doi:10.1111/jerd.12987.

107. Koban, K.C.; Perko, P.; Li, Z.; Xu, Y.; Giunta, R.E.; Alfertshofer, M.G.; Kohler, L.H.; Freytag, D.L.; Cotofana, S.; Frank, K. 3D Anthropometric Facial Imaging - A comparison of different 3D scanners. *Facial Plast Surg Clin North Am* **2022**, *30*, 149–158, doi:10.1016/j.fsc.2022.01.003.

108. Meschi, N.; Vanhoenacker, A.; Strijbos, O.; Camargo dos Santos, B.; Rubbers, E.; Peeters, V.; Curvers, F.; Van Mierlo, M.; Geukens, A.; Fieuws, S. Multi-modular bone healing assessment in a randomized controlled clinical trial of root-end

surgery with the use of leukocyte-and platelet-rich fibrin and an occlusive membrane. *Clinical Oral Investigations* **2020**, *24*, 4439–4453.

109. Mushtaq, I.; Malik, A. Evaluation of the Ochsenbein-Luebke flap technique in periapical surgery at Punjab Dental Hospital Lahore Pakistan. *J Ayub Med Coll Abbottabad* **2003** *15*, 50–53.

110. Li, H.; Guo, Z.; Li, C.; Ma, X.; Wang, Y.; Zhou, X.; Johnson, T.M.; Huang, D. Materials for retrograde filling in root canal therapy. *Cochrane Database Syst Rev* **2021**, *10*, CD005517, doi:10.1002/14651858.CD005517.pub3.

111. Barakat, S.O.; AlHawamdeh, N.I.; Marar, R. Preparation protocols and periodontal applications of platelet rich fibrin, a review. *Front Dent Med* **2026**, *7*, 1810175, doi:10.3389/fdmed.2026.1810175.

112. Kleier, D.J. The continuous locking suture technique. *J Endod* **2001**, *27*, 624–626, doi:10.1097/00004770-200110000-00006.

113. Penarrocha, M.; Sanchis, J.M.; Saez, U.; Gay, C.; Bagan, J.V. Oral hygiene and postoperative pain after mandibular third molar surgery. *Oral Surg Oral Med Oral Pathol Oral Radiol Endod* **2001**, *92*, 260–264, doi:10.1067/moe.2001.115722.

114. Hays, R.D.; Spritzer, K.L.; Schalet, B.D.; Cella, D. PROMIS®-29 v2.0 profile physical and mental health summary scores. *Qual Life Res* **2018**, *27*, 1885–1891, doi:10.1007/s11136-018-1842-3.

115. Karcioglu, O.; Topacoglu, H.; Dikme, O.; Dikme, O. A systematic review of the pain scales in adults: which to use? *Am J Emerg Med* **2018**, *36*, 707–714, doi:10.1016/j.ajem.2018.01.008.

116. Buitenhuis, M.B.; Klijn, R.J.; Rosenberg, A.; Speksnijder, C.M. Reliability of 3D stereophotogrammetry for measuring postoperative facial swelling. *J Clin Med* **2022**, *11*, 7137, doi:10.3390/jcm11237137.

117. Riley, D.S.; Barber, M.S.; Kienle, G.S.; Aronson, J.K.; von Schoen-Angerer, T.; Tugwell, P.; Kiene, H.; Helfand, M.; Altman, D.G.; Sox, H. CARE guidelines for case reports: explanation and elaboration document. *Journal of clinical epidemiology* **2017**, *89*, 218–235.

118. Aragón Niño, Í.; Castillo Pardo de Vera, J.L.d.; Rodríguez Arias, J.P.; Gutiérrez Venturini, A.; Cebrián Carretero, J.L. 3D surface scanner in Maxillofacial Surgery: State of the art. **2024**.

119. Beretta, M.; Federici Canova, F.; Zaffarano, L.; Gianolio, A. Face Scan for Ceph 3D: a green way for diagnosis in children. *Eur J Paediatr Dent* **2022**, *23*, 201–203.

120. Andlauer, R.; Wachter, A.; Schaufelberger, M.; Weichel, F.; Kuhle, R.; Freudlsperger, C.; Nahm, W. 3D-Guided Face Manipulation of 2D Images for the Prediction of Post-Operative Outcome After Cranio-Maxillofacial Surgery. *IEEE Trans Image Process* **2021**, *30*, 7349–7363, doi:10.1109/TIP.2021.3096081.

121. Aldridge, K.; Boyadjiev, S.A.; Capone, G.T.; DeLeon, V.B.; Richtsmeier, J.T. Precision and error of three-dimensional phenotypic measures acquired from 3dMD photogrammetric images. *Am J Med Genet A* **2005**, *138A*, 247–253, doi:10.1002/ajmg.a.30959.

122. Tzou, C.H.; Artner, N.M.; Pona, I.; Hold, A.; Placheta, E.; Kropatsch, W.G.; Frey, M. Comparison of three-dimensional surface-imaging systems. *J Plast Reconstr Aesthet Surg* **2014**, *67*, 489–497, doi:10.1016/j.bjps.2014.01.003.

123. Maal, T.J.; van Loon, B.; Plooij, J.M.; Rangel, F.; Ettema, A.M.; Borstlap, W.A.; Berge, S.J. Registration of 3-dimensional facial photographs for clinical use. *J Oral Maxillofac Surg* **2010**, *68*, 2391–2401, doi:10.1016/j.joms.2009.10.017.

124. Bahsi, I.; Orhan, M.; Kervancioglu, P.; Karatepe, S.; Sayin, S. Craniofacial Anthropometry of Healthy Turkish Young Adults: Analysis of Head and Face. *J Craniofac Surg* **2021**, *32*, 1535–1539, doi:10.1097/SCS.0000000000007219.

125. Zhang, S.; Zhang, S.; Fang, C.; Lan, D.; Dong, C. Application of 3-Dimensional White-Light Scanning to Observe the Lip and Nose Morphology of Chinese Children. *J Craniofac Surg* **2023**, *34*, 684–686, doi:10.1097/SCS.0000000000009040.

126. Hammond, P. The use of 3D face shape modelling in dysmorphology. *Arch Dis Child* **2007**, *92*, 1120–1126, doi:10.1136/adc.2006.103507.

127. Hajeer, M.Y.; Mao, Z.; Millett, D.T.; Ayoub, A.F.; Siebert, J.P. A new three-dimensional method of assessing facial volumetric changes after orthognathic treatment. *Cleft Palate Craniofac J* **2005**, *42*, 113–120, doi:10.1597/03-132.1.

128. Weinberg, S.M.; Naidoo, S.; Govier, D.P.; Martin, R.A.; Kane, A.A.; Marazita, M.L. Anthropometric precision and accuracy of digital three-dimensional photogrammetry: comparing the Genex and 3dMD imaging systems with one another and with direct anthropometry. *J Craniofac Surg* **2006**, *17*, 477–483, doi:10.1097/00001665-200605000-00015.

129. Maal, T.J.; Verhamme, L.M.; van Loon, B.; Plooij, J.M.; Rangel, F.A.; Kho, A.; Bronkhorst, E.M.; Berge, S.J. Variation of the face in rest using 3D stereophotogrammetry. *Int J Oral Maxillofac Surg* **2011**, *40*, 1252–1257, doi:10.1016/j.ijom.2011.02.033.

130. Singh, P.; Bornstein, M.M.; Hsung, R.T.; Ajmera, D.H.; Leung, Y.Y.; Gu, M. Frontiers in Three-Dimensional Surface Imaging Systems for 3D Face Acquisition in Craniofacial Research and Practice: An Updated Literature Review. *Diagnostics (Basel)* **2024**, *14*, doi:10.3390/diagnostics14040423.

131. Meschi, N.; Vanhoenacker, A.; Strijbos, O.; Dos Santos, B.C.; Rubbers, E.; Peeters, V.; Curvers, F.; Van Mierlo, M.; Geukens, A.; Fieuws, S.; et al. Multi-modular bone healing assessment in a randomized controlled clinical trial of root-end surgery with the use of leukocyte- and platelet-rich fibrin and an occlusive membrane. *Clin Oral Investig* **2020**, *24*, 4439–4453, doi:10.1007/s00784-020-03309-1.

132. Jenei, B.; Bato, A.; Mitev, A.Z.; Brodszky, V.; Rencz, F. Hungarian PROMIS-29+2: psychometric properties and population reference values. *Qual Life Res* **2023**, *32*, 2179–2194, doi:10.1007/s11136-023-03364-7.

133. Ramos, E.U.; Bizelli, V.F.; Baggio, A.M.P.; Ferriolli, S.C.; Prado, G.A.S.; Bassi, A.P.F. Do the new protocols of platelet-rich fibrin centrifugation allow better control of postoperative complications and healing after surgery of impacted lower third molar? A systematic review and meta-analysis. *J Oral Maxillofac Surg* **2022**, *80*, 1238–1253, doi:10.1016/j.joms.2022.03.011.

134. Tuk, J.G.; Lindeboom, J.A.; Van Wijk, A.J. Effect of periapical surgery on oral health-related quality of life in the first postoperative week using the Dutch version of oral health impact profile-14. *Oral Maxillofac Surg* **2021**, *25*, 549–559, doi:10.1007/s10006-021-00954-y.

135. Starz, F.; Valdec, S.; Lotz, M. Alveolar ridge preservation with autologous dentin following cystectomy. *Swiss Dental Journal* **2022**, *132*, 113–116.

136. Hollinger, J.O.; Kleinschmidt, J.C. The critical size defect as an experimental model to test bone repair materials. *Journal of Craniofacial Surgery* **1990**, *1*, 60–68.

137. Schlegel, K.A.; Lang, F.J.; Donath, K.; Kulow, J.T.; Wiltfang, J. The monocortical critical size bone defect as an alternative experimental model in testing bone substitute materials. *Oral Surgery, Oral Medicine, Oral Pathology, Oral Radiology, and Endodontology* **2006**, *102*, 7–13.

138. Schwenzer, N.; Ehrenfeld, M. *Zahnärztliche Chirurgie*; Georg Thieme Verlag: 2019.

139. Wiltfang, J.; Kloss, F.R.; Kessler, P.; Nkenke, E.; Schultze-Mosgau, S.; Zimmermann, R.; Schlegel, K.A. Effects of platelet-rich plasma on bone healing in combination with autogenous bone and bone substitutes in critical-size defects. An animal experiment. *Clin Oral Implants Res* **2004**, *15*, 187–193, doi:10.1111/j.1600-0501.2004.00980.x.

140. Guillaume, B.; Gaudin, C.; Georgeault, S.; Mallet, R.; Baslé, M.F.; Chappard, D. Viability of osteocytes in bone autografts harvested for dental implantology. *Biomedical Materials* **2008**, *4*, 015012.

141. Nkenke, E.; Neukam, F.W. Autogenous bone harvesting and grafting in advanced jaw resorption: morbidity, resorption and implant survival. *Eur J Oral Implantol* **2014**, *7*, S203–S217.

142. Monje, A.; Monje, F.; Hernández-Alfaro, F.; Gonzalez-García, R.; del Amo, F.S.-L.; Galindo-Moreno, P.; Montanero-Fernández, J.; Wang, H.-L. Horizontal bone augmentation using autogenous block grafts and particulate xenograft in the severe atrophic maxillary anterior ridges: a cone-beam computerized tomography case series. *Journal of Oral Implantology* **2015**, *41*, 366–371.

143. Kattimani, V.S.; Chakravarthi, S.P.; Devi, K.N.N.; Sridhar, M.S.; Prasad, L.K. Comparative evaluation of bovine derived hydroxyapatite and synthetic hydroxyapatite graft in bone regeneration of human maxillary cystic defects: a clinico-radiological study. *Indian Journal of Dental Research* **2014**, *25*, 594–601.

144. Horvathy, D.B.; Vacz, G.; Szabo, T.; Szigyarto, I.C.; Toro, I.; Vamos, B.; Hornyak, I.; Renner, K.; Klara, T.; Szabo, B.T. Serum albumin coating of demineralized bone matrix results in stronger new bone formation. *Journal of Biomedical Materials Research Part B: Applied Biomaterials* **2016**, *104*, 126–132.

145. Horváthy, D.B.; Schandl, K.; Schwarz, C.M.; Renner, K.; Hornyák, I.; Szabó, B.T.; Niculescu-Morzsa, E.; Nehrer, S.; Dobó-Nagy, C.; Doros, A. Serum albumin-coated bone allograft (BoneAlbumin) results in faster bone formation and mechanically stronger bone in aging rats. *Journal of tissue engineering and regenerative medicine* **2019**, *13*, 416–422.

146. Márton, K.; Tamás, S.B.; Orsolya, N.; Béla, C.; Ferenc, D.; Péter, N.; Csaba, D.-N.; Lajos, C.; Zsombor, L.; Eitan, M. Microarchitecture of the augmented bone following sinus elevation with an albumin impregnated demineralized freeze-Dried bone allograft (bonealbumin) versus anorganic bovine bone mineral: A randomized prospective clinical, histomorphometric, and micro-Computed tomography study. *Materials* **2018**, *11*, 202.

147. Simonffy, L.; Minya, F.; Trimmel, B.; Lacza, Z.; Dobo-Nagy, C. Albumin-Impregnated Allograft Filling of Surgical Extraction Sockets Achieves Better Bone Remodeling Than Filling with Either Blood Clot or Bovine Xenograft. *International Journal of Oral & Maxillofacial Implants* **2020**, *35*.

148. Gyulay, K.K.; Karászi, P.; Rédei, M.; Sólymos, P.; Schandl, K.; Lacza, Z.; Horváthy, D.B. Evaluation of serum albumin-coated bone allograft for bone regeneration: a seven-year follow-up study of 26 cases. *International Journal of Molecular Sciences* **2023**, *24*, 9232.

149. Choukroun, J.; Diss, A.; Simonpieri, A.; Girard, M.-O.; Schoeffler, C.; Dohan, S.L.; Dohan, A.J.; Mouhyi, J.; Dohan, D.M. Platelet-rich fibrin (PRF): a second-generation platelet concentrate. Part V: histologic evaluations of PRF effects on

bone allograft maturation in sinus lift. *Oral Surgery, Oral Medicine, Oral Pathology, Oral Radiology, and Endodontology* **2006**, *101*, 299–303.

150. Kobayashi, E.; Fluckiger, L.; Fujioka-Kobayashi, M.; Sawada, K.; Sculean, A.; Schaller, B.; Miron, R.J. Comparative release of growth factors from PRP, PRF, and advanced-PRF. *Clin Oral Investig* **2016**, *20*, 2353–2360, doi:10.1007/s00784-016-1719-1.

151. Sharma, R.; Tandan, M.; Soi, S.; Gupta, A. Surgical management of a large endodontic periapical lesion with bone putty and platelet-rich fibrin: a case report with a two-year volumetric follow-up. *Cureus* **2024**, *16*, e69355, doi:10.7759/cureus.69355.

152. Ng, Y.L.; Gulabivala, K. Factors that influence the outcomes of surgical endodontic treatment. *Int Endod J* **2023**, *56*, 116–139, doi:10.1111/iej.13896.

9. Bibliography of Candidate's Publication

9.1. Publications Directly Related to the Dissertation

MajorM., TrimmelB., PolyákM., KovácsD., & SzabóG. (2022). A Platelet Rich Fibrin szerepe a fogászatban és a maxillofaciális sebészetben: Irodalmi áttekintés. *Fogorvosi Szemle*, *115*(4), 202-206. https://doi.org/10.33891/FSZ.114.4.202-206

Major, M.; Mészáros, B.; Würsching, T.; Polyák, M.; Kammerhofer, G.; Németh, Z.; Szabó, G.; Nagy, K. Evaluation of a Structured Light Scanner for 3D Facial Imaging: A Comparative Study with Direct Anthropometry. *Sensors* **2024**, *24*, 5286. https://doi.org/10.3390/s24165286
IF: 3.5

Major, M.; Polyák, M.; Würsching, T.; Kammerhofer, G.; Kocsis, É.; Németh, Z.; Szabó, G. PRF Membranes Enhance Postoperative Recovery After Periapical Surgery: A Single-Blind Randomized Pilot Trial Using 3D Imaging. *Oral* **2025**, *5*, 98. https://doi.org/10.3390/oral5040098
IF: 1.5

Major, M.; Kivovics, M.; Szabó, B.T.; Déri, T.; Polyák, M.; Jákob, N.P.; Csete, D.; Mócsai, A.; Németh, Z.; Szabó, G. Surgical Treatment of Multiple Bone Cysts Using a Platelet-Rich Fibrin and BoneAlbumin Composite Graft: A Case Report. *Reports* **2024**, *7*, 7. https://doi.org/10.3390/reports7010007
IF: 0.6

9.2. Publications Not Related to the Dissertation

Pénzes, D.; Szerencse, C.; Major, M.; Szabó, G.; Kontsek, E.; Báskay, J.; Pollner, P.; Szabó, B.T.; Dobó-Nagy, C.; Csete, D.; et al. Microarchitectural Study of the

Augmented Bone Following a Modified Ridge Splitting Technique: Histological and Micro-Computed Tomography Analyses. *J. Clin. Med.* **2024**, *13*, 6679. https://doi.org/10.3390/jcm13226679
IF: 2.9

Turbucz, B.; Major, M.; Zelko, R.; Hanko, B. Proposal for Handling of Medicine Shortages Based on a Comparison of Retrospective Risk Analysis. *Int. J. Environ. Res. Public Health* **2022**, *19*, 4102. https://doi.org/10.3390/ijerph19074102
IF: 0

Kammerhofer, G.; Vegh, D.; Papocsi, P.; Major, M.; Fuzes, P.; Vaszilko, M.; Ujpal, M.; Haba, K.S.; Szabo, G.; Nemeth, Z. Emergency Dental Care During the SARS-CoV-2 Pandemic and Its Effect on Medication-Related Osteonecrosis of the Jaw: A Retrospective Study in Hungary. *Appl. Sci.* **2024**, *14*, 11691. https://doi.org/10.3390/app142411691
IF: 2.5

9.3. Total Cumulative Impact Factor

IF: 11

10. Acknowledgements

First and foremost, I would like to express my deepest gratitude to my supervisor, **Prof. Dr. György Szabó**, whose exceptional academic guidance, professional mentorship, and personal support have profoundly shaped the course of my scientific journey. His intellectual generosity, critical insight, and unwavering encouragement opened doors I had never imagined, and played a pivotal role not only in the progress of my research but also in my personal and professional growth. I am truly grateful for the opportunity to learn from him as a scholar, as a clinician, and as a human being.

I am deeply grateful to the institutional and departmental leaders who supported and mentored my research and generously provided the facilities and environment necessary for its execution. I would like to express my sincere thanks to **Prof. Dr. Zsolt Németh** and **Prof. Dr. Árpád Joób-Fancsaly** for their encouragement, professional guidance, and for fostering a framework in which this work could take shape.

I would also like to extend my sincere thanks to my co-authors and research collaborators, without whom neither the studies nor the resulting publications could have come to fruition. I am especially grateful to **Dr. Márton Kivovics**, **Dr. Tamás Würsching**, **Dr. Gábor Kammerhofer**, **Dr. Bence Mészáros**, and **Dr. Krisztián Nagy** for their invaluable contributions, professional insight, and dedication throughout the research process. Their collaboration and support were instrumental in transforming ideas into tangible scientific outcomes.

I would also like to acknowledge the technical and administrative support that greatly contributed to the successful completion of this work. I am especially thankful to **Dr. Éva Kocsis** for her dedicated assistance in the statistical analysis and interpretation of data. My sincere gratitude also goes to **Zsanett Szemes**, whose

committed work in graphic editing and the preparation and submission of the publications was invaluable throughout the research process.

I wish to extend my gratitude to all the staff members of the Department of Oral and Maxillofacial Surgery and Dentistry, Semmelweis University, whose support made it possible for me to devote time to scientific work alongside patient care.

I am deeply grateful to my **family and friends** for their unwavering support, encouragement, and patience throughout this journey even during the most challenging times. Their presence and belief in me were a constant source of strength.

In particular, I wish to express my sincere and heartfelt gratitude to **Dr. Melina Polyák**, whose continuous support was not only immensely helpful, but truly indispensable. Her tireless encouragement, intellectual insight, and emotional presence accompanied me throughout the entire PhD journey. She stood by me with unwavering dedication, and her example inspired me to persevere even when I doubted myself. Without her generosity, clarity, and strength, this dissertation would not have been possible. Her contribution was not only supportive it was **fundamental**.

List of tables

Table 1. *Definitions of the relevant morphometric variables.*

Table 2. *The caliper measurements of two examiners and the difference between them*

Table 3. *Mean scanner measurements.*

Table 4. *Comparison of the results measured by Examiner 1.*

Table 5. *Comparison of the results measured by Examiner 2.*

Table 6. *Comparison of the measurements times.*

Table 7. *Comparison of the measurements.*

Table 8. *Baseline (T0) quality-of-life dimensions.*

Table 9. *Baseline demographic characteristics of the PRF and control groups.*

Table 10. *Postoperative (T1, day 7 post-operation) quality-of-life dimensions.*

Table 11. *Volumetric analysis of swelling.*

Table 12. *Correlation between swelling and quality-of-life dimensions.*

Table 13. *Results of the micromorphometric analysis.*

Table 14. *Results of the histomorphometric analysis. The percentages of newly formed bone (NFB), residual graft particles (RGs), and non-mineralized tissue (NMT) were determined based on manual segmentation.*

List of figures

Figure 1. A-PRF+ membranes after centrifugation

Figure 2. (**a**) Odontogenic bone cist in the mandible, (**b**) The lesion is completly healed after augmentation with sticky bone, and after 3 months implants were placed in the augmented area.

Figure 3. 3D facial scan

Figure 4. The cephalometric reference points.

Figure 5. The EINSTAR scanner and accessories.

Figure 6. Steps and processes involved in the research.

Figure 7. CONSORT flow diagram.

Figure 8. Micro-CT scan: (**a**) horizontal section; (**b**) vertical section.

Figure 9. Histological section. Newly formed bone (NFB), residual graft particles (RGs), and non-mineralized tissue (NMT).

Figure 10. Comparison of postoperative VAS pain scores in the PRF and control groups. Error bars represent standard deviations. * indicates a statistically significant difference between groups in postoperative pain ($p = 0.034$, independent-samples t-test).